START 9613457.11H

0042303

PNL-10713
UC-721

Ferrocyanide Safety Project
Ferrocyanide Aging Studies
FY 1995 Annual Report

M. A. Lilga
E. V. Alderson
R. T. Hallen
M. O. Hogan
T. L. Hubler
G. L. Jones
D. J. Kowalski
M. R. Lumetta
G. F. Schiefelbein
M. R. Telander

September 1995

Prepared for
Westinghouse Hanford Company
Waste Tank Safety Program
with the U.S. Department of Energy
under Contract DE-AC06-76RLO 1830

Pacific Northwest Laboratory
Operated for the U.S. Department of Energy
by Battelle Memorial Institute

Battelle

OCT 1995
RECEIVED
EDMC

PNL-10713

START

DISCLAIMER

This report was prepared as an account of work sponsored by an agency of the United States Government. Neither the United States Government nor any agency thereof, nor Battelle Memorial Institute, nor any of their employees, makes **any warranty, express or implied, or assumes any legal liability or responsibility for the accuracy, completeness, or usefulness of any information, apparatus, product, or process disclosed, or represents that its use would not infringe privately owned rights.** Reference herein to any specific commercial product, process, or service by trade name, trademark, manufacturer, or otherwise does not necessarily constitute or imply its endorsement, recommendation, or favoring by the United States Government or any agency thereof, or Battelle Memorial Institute. The views and opinions of authors expressed herein do not necessarily state or reflect those of the United States Government or any agency thereof.

PACIFIC NORTHWEST LABORATORY
operated by
BATTELLE MEMORIAL INSTITUTE
for the
UNITED STATES DEPARTMENT OF ENERGY
under Contract DE-AC06-76RLO 1830

Printed in the United States of America

Available to DOE and DOE contractors from the Office of Scientific and Technical Information, P.O. Box 62, Oak Ridge, TN 37831; prices available from (615) 576-8401.

Available to the public from the National Technical Information Service, U.S. Department of Commerce, 5285 Port Royal Rd., Springfield, VA 22161

This document was printed on recycled paper.

9613457.1112

PNL-10713
UC-721

Ferrocyanide Safety Project
Ferrocyanide Aging Studies
FY 1995 Annual Report

M. A. Lilga
E. V. Alderson
R. T. Hallen
M. O. Hogan
T. L. Hubler
G. L. Jones
D. J. Kowalski
M. R. Lumetta
G. F. Schiefelbein
M. R. Telander

September 1995

Prepared for
Westinghouse Hanford Company
Waste Tank Safety Program
with the U.S. Department of Energy
under Contract DE-AC06-76RLO 1830

Pacific Northwest Laboratory
Richland, Washington 99352

THIS PAGE INTENTIONALLY
LEFT BLANK

9613457.1113

Summary

This annual report gives the results of the work conducted by the Pacific Northwest Laboratory in FY 1995 on Task 3 of the Ferrocyanide Safety Project, Ferrocyanide Aging Studies. Aging refers to the dissolution and hydrolysis of simulated Hanford ferrocyanide waste in alkaline aqueous solutions by radiolytic and chemical means. The ferrocyanide simulant primarily used in these studies was dried In-Farm-1B, Rev. 7, prepared by Westinghouse Hanford Company to simulate the waste generated when the In-Farm flowsheet was used to remove radiocesium from waste supernates in single-shell tanks at the Hanford Site. In the In-Farm flowsheet, nickel ion and ferrocyanide anion were added to waste supernates to precipitate sodium nickel ferrocyanide, $Na_2NiFe(CN)_6$, and co-precipitate radiocesium. Once the radiocesium was removed, supernates were pumped from the tanks, and new wastes from cladding removal processes or from evaporators were added. These new wastes were typically highly caustic, having hydroxide ion concentrations of over 1 *M* and as high as 4 *M*. The Aging Studies task is investigating reactions this caustic waste may have had with the precipitated ferrocyanide waste in a radiation field.

In previous Aging Studies research, $Na_2NiFe(CN)_6$ in simulants was shown to dissolve in basic solutions, forming insoluble $Ni(OH)_2$ and soluble $Na_4Fe(CN)_6$. The influence on solubility of base strength, sodium ion concentration, anions, and temperature was previously investigated. Destruction of ferrocyanide anion by hydrolysis to form ammonia and formate ion was found to be promoted by gamma irradiation. Increasing temperature and gamma dose rate increased the rate of hydrolysis, as indicated by the amount of ammonia formed with time. Ammonia was found to be radiolyzed in the gamma field. The change in concentration of formate ion generally paralleled that of ammonia but was three to four times less concentrated. Total soluble iron concentrations were found to decrease in what appeared to be a pseudo-first-order fashion. The nickel concentration tended to increase, sometimes to 90% redissolution. Aluminum added to the hydrolysis solution had relatively little effect and may have slightly promoted hydrolysis.

In FY 1995 Aging Studies work, temperature and gamma dose rate effects were further investigated. Consistent with prior work, as the temperature or the gamma dose rate increased, the rate of hydrolysis also increased. As an approximation, ammonia production with time was described as being linear. Rate constants for ammonia production followed a linear Arrhenius relationship and also increased linearly with increasing applied gamma dose rate. Rate constants for ammonia production at other conditions could be predicted with use of the temperature and dose rate relationships.

Ammonia was found to be destroyed in the gamma environment. Rate constants of 1.1×10^{-3} *M*/day at an applied dose rate of 1.07×10^5 Rad/h, and 2.1×10^{-4} *M*/day at 8.91×10^3 Rad/h were measured for this process. Formate ion destruction was found to occur at a faster rate than ammonia destruction. At an applied dose rate of 1.07×10^5 Rad/h, a rate constant for formate radiolysis of 6.15×10^{-3} *M*/day was calculated. These results are consistent with observations that the formate concentrations are much less than the ammonia concentrations in hydrolysis solutions.

The redissolved nickel species was identified as the $Ni(CN)_4^{-2}$ anion by FTIR analysis of supernate solutions. $Ni(CN)_4^{-2}$ was found to hydrolyze at a slightly slower rate than ferrocyanide anion in a gamma field.

Hydrolysis occurred faster than expected at 60°C in a pH 10 solution, considering the low solubility of $Na_2NiFe(CN)_6$ at this pH. In the gamma field, an ammonia yield of at least 18 mole% was obtained. The rate constant for ammonia production was reasonably approximated using temperature and dose rate relationships developed from experiments conducted in 2 *M* NaOH. These results may indicate that even ferrocyanide sludge that did not come into direct contact with highly basic wastes may also have aged significantly.

9613457.1114

Contents

Summary iii

Abbreviations xi

1.0 Introduction 1.1

2.0 Work Accomplished 2.1

2.1 Experimental 2.1

2.1.1 Materials and Methodology 2.2

2.1.2 Analytical Methods 2.3

2.2 Radiolysis of Ammonia and Formate Ion Under Hydrolysis Conditions 2.4

2.3 Hydrolysis of In-Farm Ferrocyanide Flowsheet Material 2.6

2.3.1 Dependence of Hydrolysis on Temperature 2.6

2.3.2 Dependence of IF-1B Hydrolysis on Gamma Dose Rate 2.14

2.3.3 Influence of Added Metal Ions on IF-1B Hydrolysis 2.19

2.4 Hydrolysis of $K_2Ni(CN)_4$ 2.21

2.5 Hydrolysis of IF-1B at 60°C and pH 10 . . . . . 2.21

3.0 Conclusions 3.1

4.0 References 4.1

THIS PAGE INTENTIONALLY
LEFT BLANK

9613457.1115

Figures

2.1 Radiolysis of Ammonia Under Hydrolysis Experiment Conditions at Gamma Dose Rates of 1.07 x 10^5 Rad/h and 8.91 x 10^3 Rad/h 2.5

2.2 Radiolysis of Formate Ion Under Hydrolysis Experiment Conditions at a Gamma Dose Rate of 1.07 x 10^5 Rad/h 2.5

2.3 Ammonia and Formate Ion Production in the Hydrolysis of IF-1B in 2 *M* NaOH at 80°C and 1.07 x 10^5 Rad/h (H10) 2.7

2.4 Ammonia and Formate Ion Production in the Hydrolysis of IF-1B in 2 *M* NaOH at 100°C and 1.07 x 10^5 Rad/h (H11) 2.8

2.5 Temperature Dependence of Ammonia Production in the Hydrolysis of IF-1B (0.5 g) at a Gamma Dose Rate of 1.07 x 10^5 Rad/h 2.9

2.6 Linear Approximation to the Temperature Dependence of Ammonia Production in the Hydrolysis of IF-1B (0.5 g) at a Gamma Dose Rate of 1.07 x 10^5 Rad/h 2.9

2.7 Eyring Plot for Ammonia Production in the Hydrolysis of IF-1B Flowsheet Material 2.11

2.8 Total Iron Concentration in the Hydrolysis of IF-1B (0.5 g) at 100°C and at a Gamma Dose Rate of 1.07 x 10^5 Rad/h (H11) 2.12

2.9 First-order Plot for the Change in Iron Concentration in the Hydrolysis of IF-1B (0.5 g) at 100°C and at a Gamma Dose Rate of 1.07 x 10^5 Rad/h (H11) 2.12

2.10 Change in Total Iron Concentration in the Hydrolysis of IF-1B (0.5 g) as a Function of Temperature at a Gamma Dose Rate of 1.07 x 10^5 Rad/h 2.13

2.11 Eyring Plot for Iron Concentration Decrease in the Hydrolysis of IF-1B Flowsheet Material 2.13

2.12 Total Nickel Concentration in the Hydrolysis of IF-1B (0.5 g) at 80°C and at a Gamma Dose Rate of 1.07 x 10^5 Rad/h (H10) 2.15

2.13 Applied Gamma Dose Rate Dependence of Ammonia Production in the Hydrolysis of IF-1B (0.5 g) at 90°C 2.16

2.14 Linear Approximation to the Applied Gamma Dose Rate Dependence of Ammonia Production in the Hydrolysis of IF-1B (0.5 g) at 90°C 2.16

2.15 Ammonia Production Rate Constant as a Function of Applied Gamma Dose Rate in the Hydrolysis of IF-1B (0.5 g) at 90°C 2.17

2.16 Decrease in Iron Concentration and Pseudo-First-Order Fit as a Function of Applied Gamma Dose Rate in the Hydrolysis of IF-1B (0.5 g) at 90°C 2.18

2.17 Iron Loss Rate Constant as a Function of Applied Gamma Dose Rate in the Hydrolysis of IF-1B (0.5 g) at 90°C 2.18

2.18 Ammonia Production During Hydrolysis of IF-1B in an Experiment in Which Both the Applied Gamma Dose Rate and Temperature Were Varied 2.19

2.19 Influence of Added Metal Ions on Hydrolysis of IF-1B at 90°C with an Applied Gamma Dose Rate of 1.07×10^5 Rad/h 2.20

2.20 Ammonia Production During Hydrolysis of $K_2Ni(CN)_4$ in 2 *M* NaOH at 90°C with an Applied Gamma Dose Rate of 1.07×10^5 Rad/h 2.22

2.21 Ammonia Production During Hydrolysis of IF-1B at pH 10 and 60°C with an Applied Gamma Dose Rate of 4.5×10^4 Rad/h 2.22

9613457.1116

Tables

2.1 Analysis of IF-1B Dissolved in 2 *M* NaOH or en/EDTA 2.2

2.2 Conditions for IF-1B Hydrolysis Experiments Investigating the Effect of Temperature Variation. 2.7

2.3 Rate Constants for Ammonia Production and Iron Loss in Hydrolysis Experiments at Various Temperatures and Applied Gamma Dose Rates 2.10

2.4 Conditions for IF-1B Hydrolysis Experiments Investigating the Effect of Applied Gamma Dose Rate Variation. 2.15

THIS PAGE INTENTIONALLY
LEFT BLANK

9613457.1117

Abbreviations

AA	atomic absorption spectroscopy
DOE	U.S. Department of Energy
EDTA	ethylenediaminetetraacetic acid
EIS	Environmental Impact Statement
en	ethylenediamine
FTIR	Fourier transform infrared spectroscopy
IC	ion chromatography
IF-1B	In-Farm-1B, Rev. 7, WHC-prepared flowsheet ferrocyanide material
ISE	ion selective electrode
SST	single-shell storage tank at Hanford
USQ	unreviewed safety question
WHC	Westinghouse Hanford Company

THIS PAGE INTENTIONALLY
LEFT BLANK

1.0 Introduction

The research performed for this project is part of an effort begun in the mid-1980s to characterize the materials stored in the single-shell waste storage tanks (SSTs) at the U.S. Department of Energy's (DOE) Hanford Site. Various radioactive wastes from defense operations have accumulated at the Hanford Site in underground waste storage tanks since the early 1940s. During the 1950s, additional tank storage space was required to support the defense mission. Hanford Site scientists developed two procedures to obtain this additional storage volume within a short time period without constructing more storage tanks. One procedure involved the use of evaporators to concentrate the waste by removing water. The other procedure involved developing precipitation processes for scavenging radiocesium and other soluble radionuclides from tank waste liquids.

In the radiocesium scavenging processes, waste solutions were adjusted to a pH between 8 and 10; and sodium or potassium ferrocyanide and nickel sulfate were added to co-precipitate cesium with the insoluble alkali-metal nickel ferrocyanide. Because waste solutions had high nitrate and radiolytically produced nitrite concentrations, these ions became incorporated into the precipitates. After the radioactive precipitates settled, the decontaminated solutions were pumped to disposal cribs, thereby providing the additional tank storage volume. Much later, some of the tanks were "stabilized" against leakage by removing pumpable liquids from the tanks, leaving behind a wet solid (sludge) residue containing the ferrocyanide precipitates (Burger et al. 1991). In implementing this process, approximately 140 metric tons of ferrocyanide [calculated as $Fe(CN)_6^{-4}$] were added to waste that was later routed to 20 large (500,000- to 750,000-million-gal) underground SSTs. Records at Hanford show 18 SSTs contain at least 200 kg (1000 g-mol) of ferrocyanide precipitates. The ferrocyanide content of the individual tanks ranges from 200 kg up to possibly 16,600 kg in Tank BY-104 (Borsheim and Simpson 1991).

Three flowsheets were used to scavenge the radiocesium from aqueous wastes. The T-Plant flowsheet, used to treat first-cycle waste from the bismuth phosphate process, generated about 8% of the total ferrocyanide waste. The U-Plant flowsheet treated "metal waste" dissolved in nitric acid after the uranium had been recovered using the tributyl phosphate process. The U-Plant flowsheet produced about 66% of the total ferrocyanide waste. The third process, the In-Farm flowsheet, treated the basic waste from recovery of uranium. This process produced the remaining 26% of the total ferrocyanide waste.

Unlike the In-Farm flowsheet waste, T-Plant and U-Plant flowsheet waste contained substantial metal concentrations that precipitated when neutralized with sodium hydroxide. The ferrocyanide was thereby diluted, assuming that the solids-settling behaviors of the metal species and ferrocyanides were approximately the same. Although the In-Farm flowsheet produced only about a quarter of the ferrocyanide waste, the concentration of ferrocyanide in the waste is anticipated to be significantly higher than that in the T-Plant and U-Plant waste. Prepared In-Farm and U-Plant flowsheet simulants, which are representative of these wastes, contain about 25 wt% and 8 wt% ferrocyanide ion (dried simulants), respectively.

As part of waste management operations, after the ferrocyanide waste was precipitated and the supernate removed, aluminum decladding waste and/or evaporator bottoms from the concentration of reprocessing wastes were added to the tanks (Anderson 1990). These solutions were generally quite alkaline, containing NaOH concentrations of 1 to 2 *M*, with occasional additions of up to 4 *M* NaOH.

Concern has been raised about the safe storage of ferrocyanide waste intermixed with oxidants, such as nitrate and nitrite salts. In the laboratory, such mixtures can be made to undergo uncontrolled or explosive reactions by heating dry reagents to over 200°C. For example, mixtures of cesium zinc ferrocyanide and nitrate explode when heated (Hepworth et al. 1957). The 1987 Environmental Impact Statement (EIS), *Final Environmental Impact Statement, Disposal of Hanford Defense High-Level Transuranic and Tank Waste, Hanford Site, Richland, Washington* (DOE 1987), included an environmental impact analysis of potential explosions involving ferrocyanide-nitrate mixtures. The EIS postulated that an explosion could occur during mechanical retrieval of saltcake or sludge from a ferrocyanide waste tank. The EIS concluded that this worst-case accident could create enough energy to release radioactive material to the atmosphere through ventilation openings, exposing persons offsite to a short-term radiation dose of approximately 200 mrem. A General Accounting Office study (Peach 1990) postulated a greater worst-case accident, with independently calculated doses of one to two orders of magnitude greater than that postulated in the DOE EIS. Uncertainties regarding the safety envelope of the Hanford Site ferrocyanide waste tanks led to the declaration of the ferrocyanide unreviewed safety question (USQ) in October 1990 (Deaton 1990). A special Hanford Ferrocyanide Task Team was commissioned to address all technical aspects involving SSTs containing ferrocyanide wastes. The Hanford Ferrocyanide Task Team is composed of technical experts from Westinghouse Hanford Company (WHC), Pacific Northwest Laboratory[(a)], and outside consultants.

Numerous studies conducted by the Task Team resulted in closure of the USQ in March 1994. The potential for ferrocyanide reactions in Hanford Site SSTs was evaluated, and the energy released during these reactions was quantified (Burger 1984; Burger and Scheele 1988, 1991; Cady 1993; Hallen et al. 1992; Scheele and Cady 1992; Scheele et al. 1991, 1992). Recently, dynamic X-ray diffraction has been used to identify specific reactions and to quantify reaction rates (Dodds and Thompson 1994). In addition, a number of experimental and theoretical studies have been conducted in an effort to analyze the thermal characteristics of the tanks (Crowe et al. 1993; McLaren 1993, 1994; McLaren and Cash 1993) and to investigate the likelihood of "hot spots" forming as a result of radiolytic heating (Epstein and Fauske 1994; McGrail et al. 1993). The measured temperatures in these tanks continue to drop, and the highest temperature currently recorded is 53°C (Meacham et al. 1994a).

Safety criteria for ferrocyanide waste are based on the results of thermal reactivity, tank characterization, and theoretical studies (Postma et al. 1994). The most important criteria are the concentration of ferrocyanide in the waste, the amount of free (unbound) water present, and the temperature of the waste. Waste is considered safe if it contains less than 8 wt% $Na_2NiFe(CN)_6$ (measured in dried waste with no free water), regardless of temperature, water content, or oxidant content. Ferrocyanide waste

---

(a) Operated for the U.S. Department of Energy by Battelle Memorial Institute under Contract DE-AC06-76RLO 1830.

is said to be conditionally safe if it contains more than 8 wt% $Na_2NiFe(CN)_6$, contains up to 24 wt% free water, and is at a temperature less than 90°C. Tanks are categorized as unsafe if they contain higher ferrocyanide concentrations without adequate free water or contain waste at a temperature higher than 90°C. Two ferrocyanide-containing tanks are classified safe, and the rest are classified conditionally safe. None fall in the category of unsafe. Resolving the ferrocyanide safety issue requires that tank contents meet the safety criteria and operations be conducted such that waste conditions fall within the criteria limits.

Because the ferrocyanide sludge has been exposed for many years to other highly caustic wastes, as well as to elevated temperatures and both gamma and beta radiation, ferrocyanide decomposition may have occurred in the tanks. As a result, the concentration of ferrocyanide may be much less than that predicted by tank inventory records. If so, tanks may then be re-categorized as safe, facilitating remediation.

The goal of the Ferrocyanide Aging Studies task (Task 3 of the Ferrocyanide Safety Project) is to understand the long-term chemical and radiolytic behavior of ferrocyanide tank wastes in the SST environments. In turn, this information provides baseline data that will be useful as actual SST samples are obtained and analyzed. The results of Aging Studies will directly assist in determining which strategy will ensure safe storage of the ferrocyanide waste in the tanks and how the ferrocyanide safety issue can be resolved. In previous ferrocyanide waste aging studies utilizing flowsheet simulants (Lilga et al. 1992, 1993, 1994), redissolution of $Na_2NiFe(CN)_6$ in caustic solutions was shown to occur and was studied under a variety of conditions. Products of the dissolution are soluble $Fe(CN)_6^{-4}$ and insoluble $Ni(OH)_2$. Destruction of $Fe(CN)_6^{-4}$ by hydrolysis was also demonstrated.

This report describes the results of FY 1995 research for the Aging Studies task, which focused on the hydrolysis of ferrocyanide waste simulants in aqueous base. Hydrolysis was investigated in 2 *M* NaOH as a function of temperature, applied gamma dose rate, and added metal ion. A long-term hydrolysis experiment was conducted at pH 10 and 60°C. In addition, experiments investigating the hydrolysis of $K_2Ni(CN)_4$ were conducted.

THIS PAGE INTENTIONALLY
LEFT BLANK

2.0 Work Accomplished

The Aging Studies task has addressed issues regarding how ferrocyanides in tank waste may have changed over decades of storage and after additions of other highly caustic wastes. Aging, as used here, is any process that may have altered the chemical nature of the ferrocyanide waste. In these studies, the primary aging routes that have been investigated are dissolution of alkali metal nickel ferrocyanides, shown in Eq. (1) for the sodium compound, and hydrolysis of ferrocyanide ion, shown in Eq. (2) for one reported stoichiometry (Robuck and Luthy 1989).

$$Na_2NiFe(CN)_{6\,(s)} + 2\,OH^- \rightleftarrows Fe(CN)_6^{-4} + 2\,Na^+ + Ni(OH)_{2\,(s)} \quad (1)$$

$$Fe(CN)_6^{-4} + 2\,OH^- + 11\,H_2O + 1/6\,O_2 \rightarrow 6\,NH_3 + 6\,HCO_2^- + 1/3\,Fe_3O_{4\,(s)} \quad (2)$$

Research conducted in FY 1995, a continuation of research completed from FY 1992 through FY 1994, focused on the destruction of ferrocyanide anion by hydrolysis in caustic solution under conditions approximating those in SSTs. Further experiments investigating the influence of gamma dose rate, temperature, and metal ion additives on hydrolysis of an In-Farm flowsheet simulant in 2 *M* NaOH were conducted. Radiolysis of ammonia and formate ion, both of which are cyanide hydrolysis products, was studied. A series of experiments in which hydrolysis was carried out over a 6-month period at pH 10 and 60°C in a gamma field were completed. In addition, the presence of $Ni(CN)_4^{-2}$ was verified by Fourier transform infrared spectroscopy (FTIR) analysis, and the hydrolysis of this species was independently investigated. The $Ni(CN)_4^{-2}$ anion apparently forms when free cyanide ion, liberated as $Fe(CN)_6^{-4}$ is destroyed, reacts with $Ni(OH)_2$ (Eqs. 3 and 4). Other aspects of alkali metal nickel ferrocyanide solubility, including the insolubility of the cesium-containing materials, and hydrolysis have been described in previous reports (Lilga et al. 1992, 1993, 1994). In addition, mechanisms of contacting deep sludges layers with caustic have been discussed (McGrail et al. 1993; McGrail 1994).

$$Fe(CN)_6^{-4} + x\,L^n \rightleftarrows Fe(CN)_{6-x}L^{-4+x(n+1)} + x\,CN^- \quad (3)$$

$L^n = OH^-, H_2O$, etc.

$$Ni(OH)_{2\,(s)} + 4\,CN^- \rightleftarrows Ni(CN)_4^{-2} + 2\,OH^- \quad (4)$$

2.1 Experimental

This section describes the In-Farm flowsheet materials studied and summarizes the experimental methodology and the analytical methods used. A discussion of the gamma facility, the gamma dose

rate cross section experienced by irradiated solutions, and other experimental and analytical details have previously been published (Lilga et al. 1994).

2.1.1 Materials and Methodology

The ferrocyanide-containing material used in hydrolysis studies was the In-Farm-1B, Rev 7 (IF-1B) flowsheet material prepared by WHC (Jeppson and Wong 1993) and dried to constant weight at 60°C under vacuum. Atomic absorption spectroscopy (AA) analyses of dried IF-1B dissolved in 2 *M* NaOH or aqueous 5% ethylenediamine (en)/5% ethylenediaminetetraacetic acid (EDTA) at room temperature are summarized in Table 2.1. The en/EDTA solvent dissolved all of the IF-1B starting material, while the NaOH solution did not. As previously discussed, aqueous NaOH does not dissolve "$Cs_2NiFe(CN)_6$" or other phases containing cesium (Bryan et al. 1993; Lilga et al. 1993), and this insoluble phase also prevents dissolution of a fraction of the $Na_2NiFe(CN)_6$ phase. The AA analytical results for iron correspond to soluble ferrocyanide ion. Thus, at room temperature, 0.5 g of IF-1B dissolved in 25 mL of 2 *M* NaOH result in a ferrocyanide ion concentration of 0.0127 *M*. Ferrocyanide ion concentrations in the starting solutions of the hydrolysis experiments are slightly higher than the predicted concentrations based on the room temperature 2 *M* NaOH dissolution results shown in Table 2.1 because of the higher temperatures involved. For example, preliminary results at 70°C indicate that the starting ferrocyanide ion concentration for 0.5 g of IF-1B dissolved in 25 mL of 2 *M* NaOH is about 0.0155 *M*. Further experiments to determine equilibrium concentrations at reaction temperatures are now being conducted. In this report, yields are calculated based on the room-temperature solubilities.

Three different vessel styles were used in different series of experiments, as described below. Different vessels were used primarily because the number of experimental parameters requiring examination and the length of time required for each test necessitated concurrent, rather than sequential, testing. Experiments within each series were performed consistently, and results are directly comparable. Because of the length of time required for each experiment and gamma facility scheduling, relatively few duplicate experiments were possible. Duplicates were run in the metal ion testing described below. In these tests, an overall relative standard deviation of about 11% was obtained, which indicates the reproducibility of these experiments.

Table 2.1. Analysis of IF-1B Dissolved in 2 *M* NaOH or en/EDTA

Dissolving Medium	moles Fe/g IF-1B	moles Cs/g IF-1B	moles Ni/g IF-1B
2 *M* NaOH	6.35×10^{-4}	$< 7.31 \times 10^{-7}$	1.49×10^{-5}
en/EDTA	9.56×10^{-4}	3.69×10^{-5}	1.10×10^{-3}

In a typical hydrolysis experiment, identical Inconel vessels (0.23-cm wall thickness) were charged with IF-1B and argon-purged caustic solution, sealed, and pressurized and vented two times with argon. Vessels were lowered into separate tubes in the gamma pit for irradiation and brought to the desired temperature. Solutions were not stirred. Reaction vessels were individually removed from the gamma pit, usually after 2, 6, 12, 16, and 19 days. Control experiments, which were prepared and treated identically but did not undergo gamma irradiation, were normally terminated after 12 and 19 days of reaction. After termination, a gas sample was taken for mass spectral analysis. The supernate was sampled (5 mL, unfiltered) and analyzed for solution NH_3. Another 5 to 7 mL were filtered through a 0.45-μm Gelman Acrodisc syringe filter for AA, ion chromatography (IC), and FTIR analyses. The remaining supernate was filtered through a 0.47-μm magna nylon millipore filter, and the precipitate washed with de-ionized water. Precipitates were dried at 100°C. These experiments were labeled H1 through H12.

Hydrolysis experiments investigating the effect of added metal ions that are found in SST waste were conducted in essentially the same manner with the following variations. The time dependence of hydrolysis was not investigated; experiments containing metal ions were usually run for 13 days. The Inconel vessels used had a smaller inside diameter and a thicker wall thickness (0.93-cm wall thickness) than those used in the experiments described above. As a result, the geometry of the 25 mL of solution in the gamma field was different. Convective solution mixing in these unstirred solutions was also expected to be quite different. In addition, the thicker vessel wall attenuated the gamma field to a larger extent than in the thin-wall vessels, which affected the extent of hydrolysis that occurred. Therefore, while metal ion testing experiments are internally consistent, the results are not directly comparable to the normal hydrolysis experiments described above. However, experiments conducted in the thick-wall vessels in FY 1994 without metal ion additives, run for varying lengths of time, established the baseline hydrolysis behavior for comparison.

In long-term (5.3 months) radiolysis experiments conducted at 60°C with pH 10 solutions, Monel vessels were used. The wall thickness of the vessels was 0.55 cm.

2.1.2 Analytical Methods

Several different analytical methods were used to identify and quantitate hydrolysis products. Gas samples from the headspace of the hydrolysis reaction vessels were obtained with an evacuated 75-mL sample vessel through a specially prepared gas sampling/pressure monitoring panel. Gas samples were analyzed on a high-sensitivity Finnigan MAT-271 mass spectrometer for several gases, including argon, hydrogen, nitrogen, oxygen, and nitrogen oxides. The estimate of precision is better than 0.1 mole%.

Syringe-filtered hydrolysis supernates were analyzed by AA for total soluble iron, nickel, and cesium. These analyses are accurate to within 10%. The supernates were also analyzed for NO_3^-, NO_2^-, and HCO_2^- by IC, which is accurate to 5%, and for metal cyanides with FTIR spectroscopy. Dissolved ammonia was determined with use of an Orion 720A pH/ISE (ion selective electrode) meter

equipped with an Orion 95-12 NH_3 ISE. Calibration measurements were typically within 3% of the actual concentration. With the use of standard ammonia solutions, it was determined that gas phase ammonia contributed insignificantly to the overall ammonia balance; the solution ammonia concentration accounts for the ammonia in each sample. It was also determined that adsorption of ammonia on the stainless steel tubing and other surfaces in the reaction vessels and gas handling systems was insignificant. Other control experiments have shown that no ammonia is produced by radiolysis or thermolysis of nitrate and nitrite solutions under the conditions of the aging studies experiments (Lilga et al. 1994).

2.2 Radiolysis of Ammonia and Formate Ion Under Hydrolysis Conditions

Hydrolysis of ferrocyanide ion present in IF-1B produces, along with other products, ammonia and formate ion. Both of these products were found to be destroyed in the gamma field, and experiments were performed to estimate their rate of destruction under hydrolysis conditions. A set of experiments were conducted in which solutions containing either 0.03 *M* formate ion or 0.03 *M* ammonia (generated from NH_4Cl and base) along with 2 *M* NaOH, 0.095 *M* $NaNO_3$, and 0.036 *M* $NaNO_2$ were heated to 90°C and exposed to gamma radiation. Concentrations of these species were chosen to mimic the concentrations present in IF-1B hydrolysis experiments. Vessels were individually pulled from the gamma tubes after various reaction times, then analyzed.

The results of ammonia radiolysis experiments conducted with applied gamma dose rates of 1.07×10^5 Rad/h and 8.91×10^3 Rad/h are shown in Figure 2.1. Destruction appears to be a 0-order process, but there is a great deal of scatter in the data, especially at the higher dose rate after long reaction times. Radiolysis is more rapid at the higher dose rate; assuming a 0-order relationship, the destruction rate at the incident dose rate of 1.07×10^5 Rad/h is about 1.1×10^{-3} *M*/day and is about 2.1×10^{-4} *M*/day at 8.91×10^3 Rad/h.

Formate ion radiolysis is more rapid than ammonia radiolysis. Before 6 days of reaction at a dose rate of 1.07×10^5 Rad/h, formate ion is completely destroyed (Figure 2.2). Assuming destruction occurs by a 0-order process, a rate of 6.15×10^{-3} *M*/day, or over 5 times the rate of ammonia destruction, is calculated. This series of experiments, however, does not confirm 0-order destruction, and the mechanism is likely more complicated than this assumption implies (Goldstein et al. 1988).

Because ammonia is destroyed with time, mole% conversion based on ammonia only approximates the amount of cyanide or ferrocyanide hydrolyzed. Reported mole% conversion values (sometimes called apparent % conversion in this report) do not take into account the amount of ammonia lost to radiolysis.

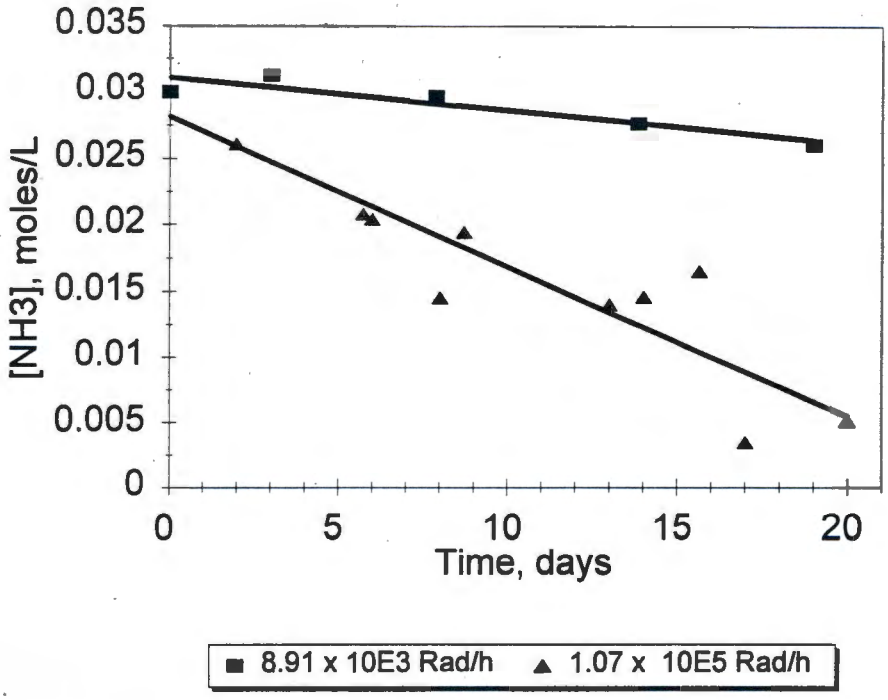

Figure 2.1. Radiolysis of Ammonia Under Hydrolysis Experiment Conditions at Gamma Dose Rates of 1.07 x 10^5 Rad/h and 8.91 x 10^3 Rad/h

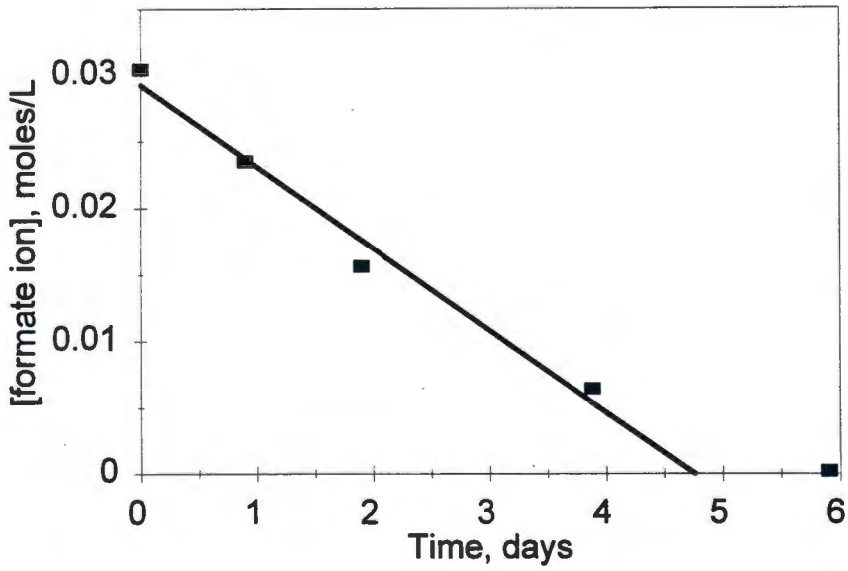

Figure 2.2. Radiolysis of Formate Ion Under Hydrolysis Experiment Conditions at a Gamma Dose Rate of 1.07 x 10^5 Rad/h

2.3 Hydrolysis of In-Farm Ferrocyanide Flowsheet Material

Experiments were conducted in 2 *M* NaOH solution to further investigate the influence of temperature and gamma dose rate on the hydrolysis of IF-1B flowsheet material. The effects of metal ions on hydrolysis were determined. Hydrolysis of $Ni(CN)_4^{2-}$ was investigated for comparison to hydrolysis of $Fe(CN)_6^{4-}$ because this nickel species was shown by FTIR to be an intermediate in the reaction. Hydrolysis at pH 10 and 60°C was studied over a 5.3-month period.

2.3.1 Dependence of Hydrolysis on Temperature

Table 2.2 summarizes conditions of experiments in which temperature was the investigated variable. Experiments H1 (90°C), H2 (70°C), and H3 (50°C) were conducted in FY 1994. Experiments H10 (80°C) and H11 (100°C) were conducted in FY 1995 because conversions at 50°C and 70°C were low, and more temperature data were needed to establish the temperature dependence. This temperature range is representative of present and past conditions in the tanks (Meacham et al. 1994b).

Figures 2.3 and 2.4 show ammonia and formate produced by hydrolysis in the gamma-irradiated and thermal (control) experiments at 80°C (H10) and 100°C (H11), respectively. The ammonia data clearly show that both temperature and gamma radiation promote the hydrolysis reaction, as observed previously in other hydrolysis experiments (Lilga et al. 1994). Ammonia concentrations in the gamma experiments are on the order of 3 to 4 times the measured formate ion concentrations. These products should be formed in a 1:1 mole ratio. However, the difference in concentrations is consistent with stoichiometric product formation followed by radiolysis as discussed in Section 2.2. The lower formate ion concentrations occur because formate ion radiolysis is more rapid than ammonia radiolysis by about a factor of 5. This conclusion is supported by data from the non-irradiated control experiments, reported here and previously, which show that the expected 1:1 mole ratio is obtained in thermal hydrolysis.

Ammonia production in the 100°C experiment appeared to proceed to over 100 mole% conversion. This is because the percent conversion was approximated based on the room-temperature solubility of the IF-1B flowsheet material in 2 *M* NaOH. The expected maximum yield of ammonia using this assumption was six times the ferrocyanide ion concentration (0.0127 *M*) or 0.0762 *M*. Two factors appear to contribute to making the observed ammonia concentration higher after 17 days at 100°C: the equilibrium solubility was probably higher than assumed, and hydrolysis of the less-soluble, cesium-containing ferrocyanide phase may have occurred to a greater extent at this temperature. The Fe/Cs molar ratio in the solids that are insoluble in 2 *M* NaOH is calculated to be 8.7 (Table 2.1), which is much higher than if all of the cesium were present as "$Cs_2NiFe(CN)_6$" (Fe/Cs = 0.5) or "$CsNaNiFe(CN)_6$" (Fe/Cs = 1.0). The insoluble material must contain the soluble $Na_2NiFe(CN)_6$ phase imbedded within the less-soluble cesium phase. Higher temperatures likely release more of the

Table 2.2. Conditions for IF-1B Hydrolysis Experiments Investigating the Effect of Temperature Variation. Experiments were conducted in 25 mL of 2 *M* NaOH for 3 weeks.

Experiment Number	Incident Gamma Dose Rate (Rad/h)	Weight IF-1B used (g)	Temperature (°C)
H11	1.07×10^5	0.5	100
H1	1.07×10^5	0.5	90
H10	1.07×10^5	0.5	80
H2	1.07×10^5	0.5	70
H3	1.07×10^5	0.5	50

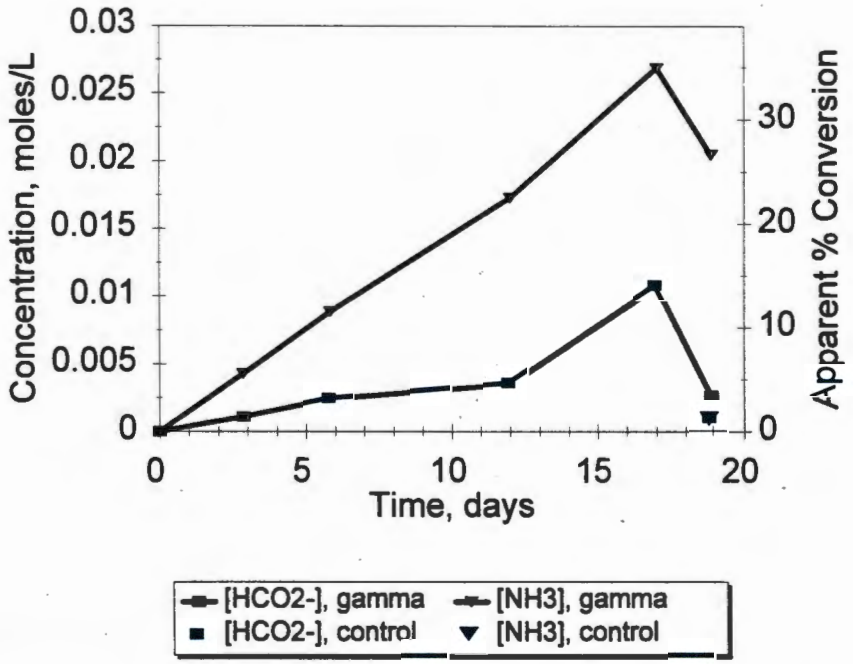

Figure 2.3. Ammonia and Formate Ion Production in the Hydrolysis of IF-1B in 2 *M* NaOH at 80°C and 1.07×10^5 Rad/h (H10). Control experiments were identical but not irradiated.

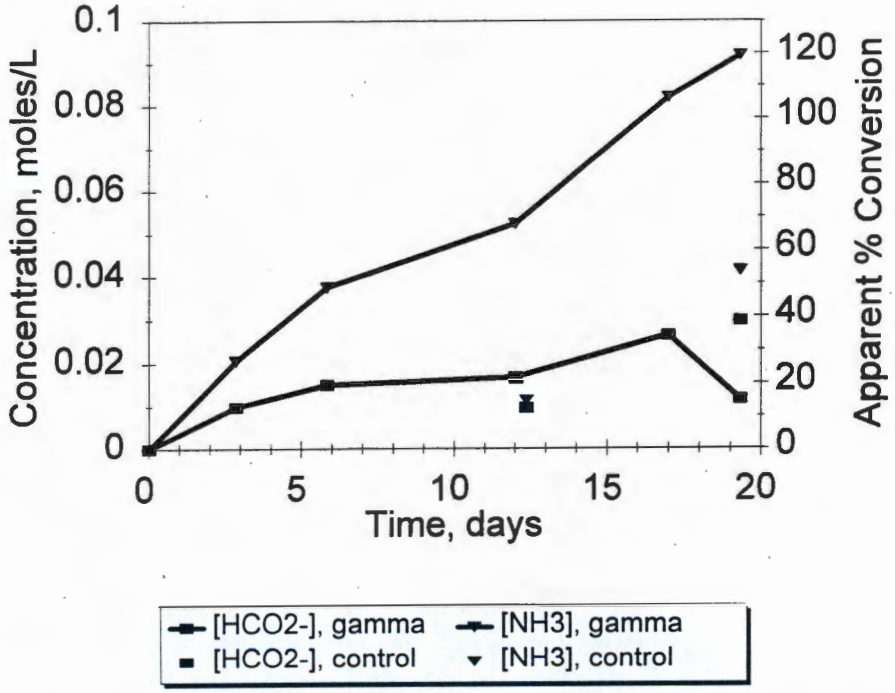

Figure 2.4. Ammonia and Formate Ion Production in the Hydrolysis of IF-1B in 2 *M* NaOH at 100°C and 1.07 x 10^5 Rad/h (H11). Control experiments were identical but not irradiated.

soluble material, as evidenced by the preliminary results which show a higher ferrocyanide ion concentration at 70°C than at room temperature. Also, cesium concentrations in supernates were highest in experiments showing extensive hydrolysis, suggesting some destruction of the initially insoluble phase occurred.

The 80°C and 100°C data for ammonia production are compared in Figure 2.5 with previously reported and some newly collected data for experiments at 50°C, 70°C, and 90°C. Overall, the ammonia concentration increased approximately linearly with hydrolysis time. This behavior was different from published thermal hydrolysis rate data, which indicated that hydrolysis was first order in total cyanide (Robuck and Luthy 1989). As an approach toward a mathematical model, the linear approximation was made (Figure 2.6) and global rate constants calculated from the slopes of the lines (Table 2.3). The Eyring plot of these rate data, shown in Figure 2.7, was linear, and an activation energy of ΔH = 32.5 kcal/mole was calculated. Rate constants for ammonia production at a given temperature at a gamma dose rate of 1.07 x 10^5 Rad/h may be calculated with use of Eq. (5). The calculated rate constants do not directly represent the rate of ferrocyanide hydrolysis because the rate of ammonia radiolysis is included. Rate constants predicted from this equation are generally within a factor of about 2 of the observed rate constants.

$$\ln(k_T/T) = 33.1 - 1.64 \times 10^4 \cdot 1/T \qquad (5)$$

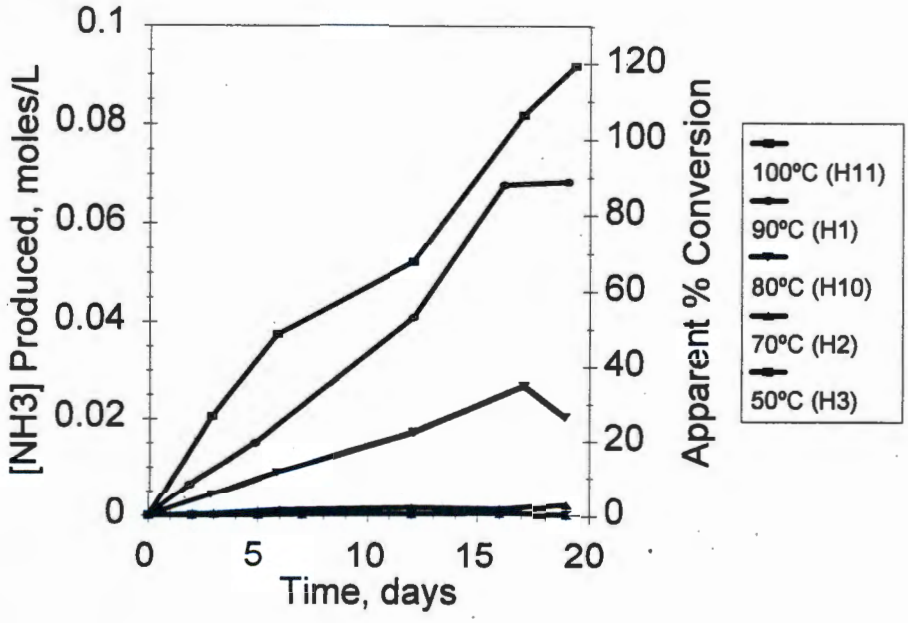

Figure 2.5. Temperature Dependence of Ammonia Production in the Hydrolysis of IF-1B (0.5 g) at a Gamma Dose Rate of 1.07 x 10^5 Rad/h

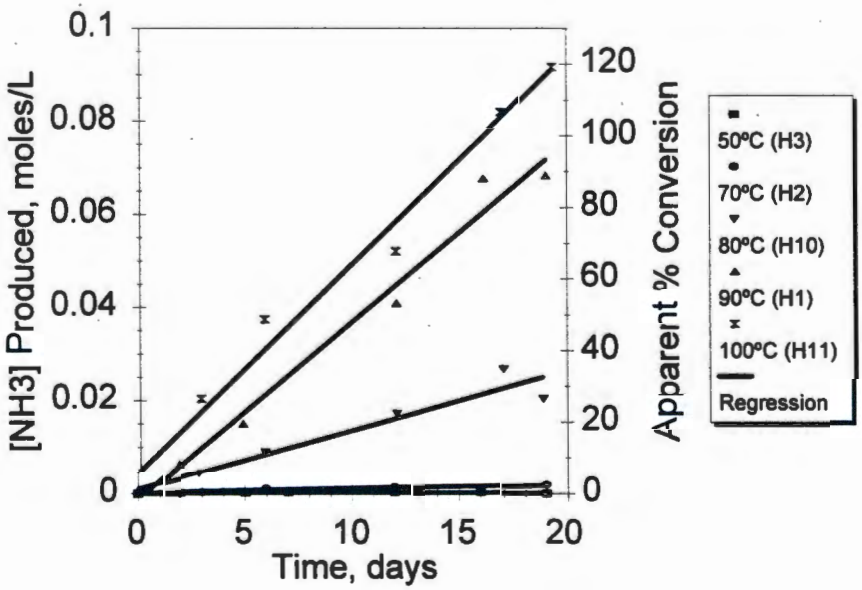

Figure 2.6. Linear Approximation to the Temperature Dependence of Ammonia Production in the Hydrolysis of IF-1B (0.5 g) at a Gamma Dose Rate of 1.07 x 10^5 Rad/h

Table 2.3. Rate Constants for Ammonia Production and Iron Loss in Hydrolysis Experiments at Various Temperatures and Applied Gamma Dose Rates

Experiment Number	Temperature (°C)	Applied Gamma Dose Rate (Rad/h)	NH_3 Production Rate Constant (*M*/day)	Iron Loss Rate Constant (day^{-1})
H3	50	1.07×10^5	7.76×10^{-6}	-
H2	70	1.07×10^5	8.87×10^{-5}	0.022
H10	80	1.07×10^5	1.28×10^{-3}	0.078
H1	90	1.07×10^5	3.83×10^{-3}	0.11
H11	100	1.07×10^5	4.47×10^{-3}	0.22
H4	90	4.25×10^4	1.99×10^{-3}	0.060
H5	90	8.91×10^3	1.05×10^{-3}	0.0025

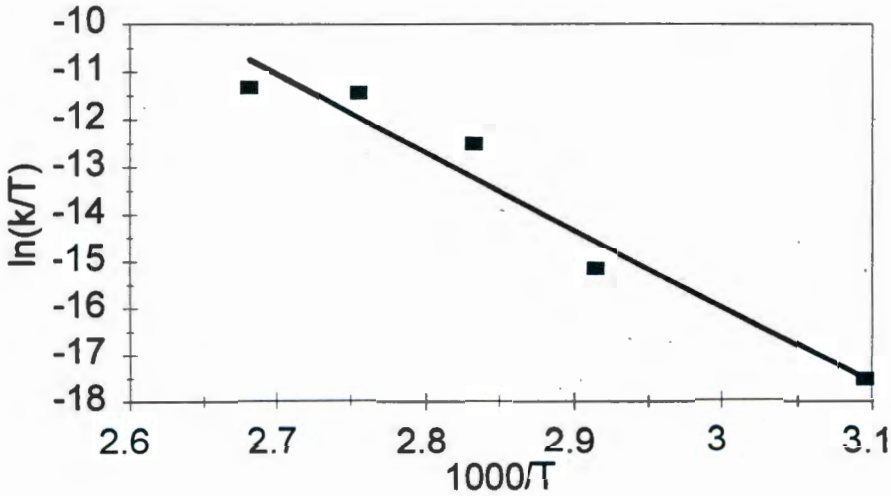

Figure 2.7. Eyring Plot for Ammonia Production in the Hydrolysis of IF-1B Flowsheet Material

The change in soluble iron concentration (as determined by AA) for the experiment at 100°C and 1.07 x 10^5 Rad/h (H11) is shown in Figure 2.8. The observed data, shown as data points, are a measure of all soluble iron species. The line in the figure represents a pseudo-first-order fit to all of the data from the gamma-irradiated experiments. The rate constant of 0.22 day^{-1} was determined from the slope of the line in a plot of ln[Fe] versus time (Figure 2.9). The rate constant is a pseudo-first-order rate constant since the loss of soluble iron from solution likely involves reaction with hydroxide, present in large excess, to precipitate iron hydroxides or oxides.

Figure 2.10 compares iron loss at 70°C, 80°C, 90°C, and 100°C. Lines show the fit to the data assuming pseudo-first-order iron loss at each temperature. The first-order assumption is based on the 100°C data, but, at lower temperatures, this is not a unique model that describes the data. For example, the decrease in iron concentration might be described just as accurately as being linear in some of the experiments. Calculated pseudo-first-order rate constants are shown in Table 2.3, and the Eyring plot is shown in Figure 2.11. The activation energy for iron loss from solution is 17.6 kcal/mole.

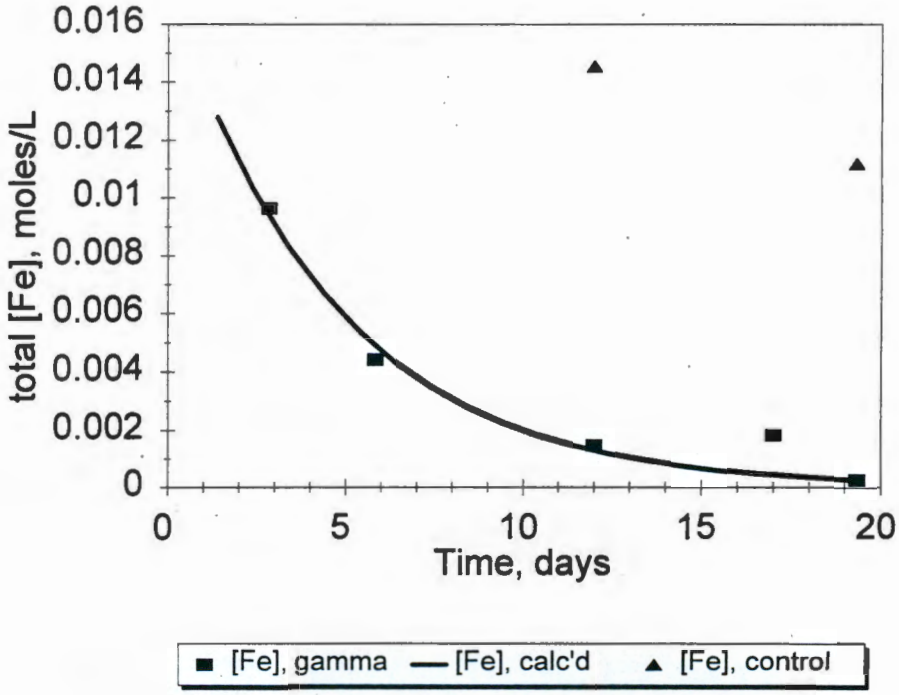

Figure 2.8. Total Iron Concentration in the Hydrolysis of IF-1B (0.5 g) at 100°C and at a Gamma Dose Rate of 1.07 x 10^5 Rad/h (H11)

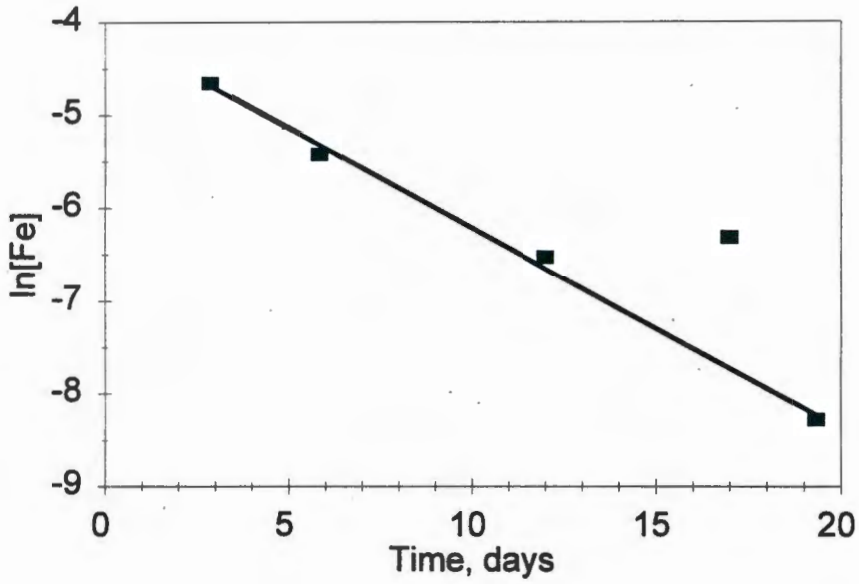

Figure 2.9. First-order Plot for the Change in Iron Concentration in the Hydrolysis of IF-1B (0.5 g) at 100°C and at a Gamma Dose Rate of 1.07 x 10^5 Rad/h (H11)

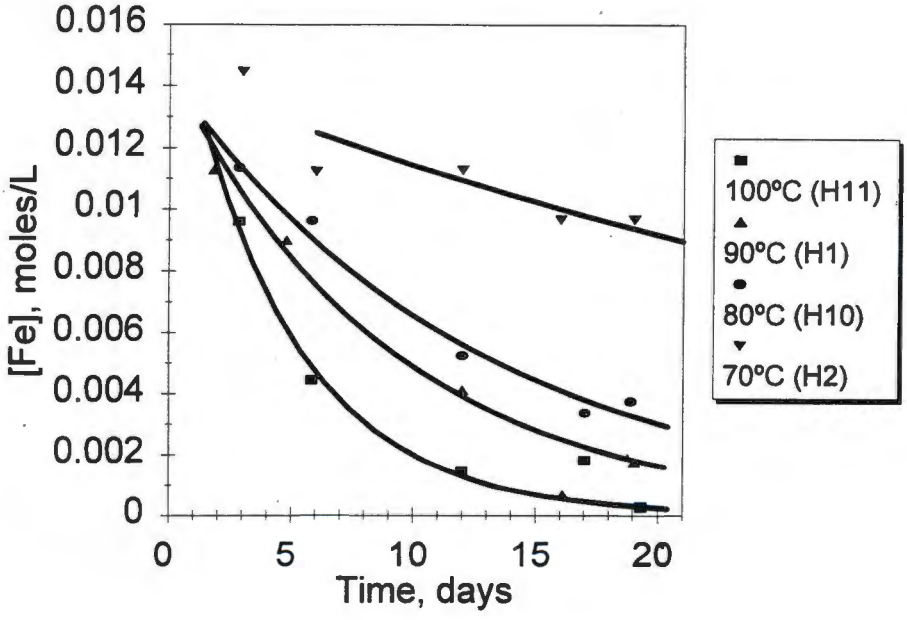

Figure 2.10. Change in Total Iron Concentration in the Hydrolysis of IF-1B (0.5 g) as a Function of Temperature at a Gamma Dose Rate of 1.07 x 10^5 Rad/h

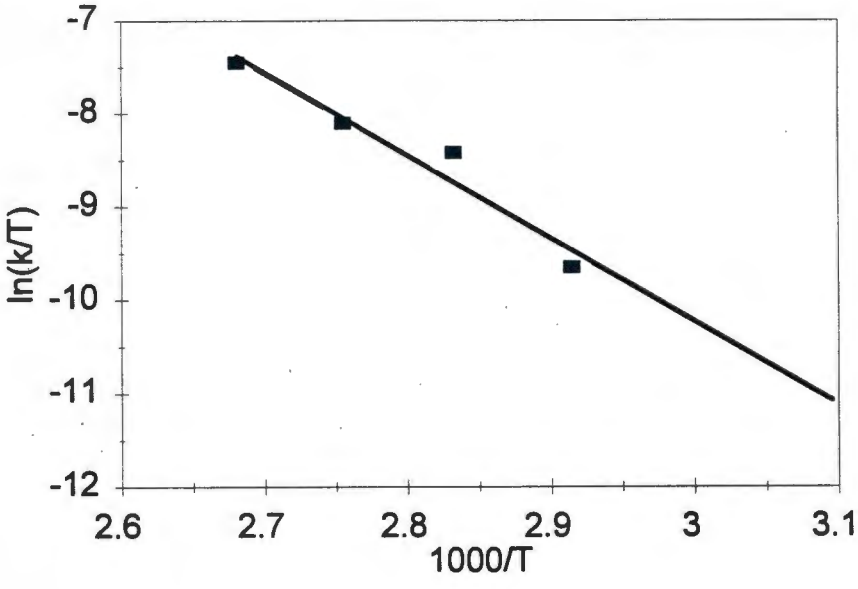

Figure 2.11. Eyring Plot for Iron Concentration Decrease in the Hydrolysis of IF-1B Flowsheet Material

Infrared spectra of gamma-irradiated supernates from selected experiments showed that the dissolved iron consisted of the $Fe(CN)_6^{-4}$ anion (2037 cm^{-1}). The concentrations of ferrocyanide ion from the FTIR results were in very good agreement with the total iron concentrations determined by AA analysis.

FTIR spectra of supernate samples from the same selected experiments also often showed the presence of $Ni(CN)_4^{-2}$ (2123 cm^{-1}). This species was identified by comparison of its spectrum with that of a commercial sample. In addition, the calculated concentrations of this species by FTIR matched the total nickel concentrations determined by AA. Formation of this species was responsible for the nickel redissolution phenomenon observed previously and shown in Figure 2.12 for the 80°C, 1.07 x 10^5 Rad/h (H10) experiment. After 19 days, over 90% of the nickel was in solution as $Ni(CN)_4^{-2}$.

Initially, $Ni(OH)_2$ precipitates when aqueous base is added to the flowsheet material, which contains $Na_2NiFe(CN)_6$. As hydrolysis takes place, cyanide ion is liberated from iron. Some of the cyanide is converted to ammonia and formate ion, and some survives to redissolve nickel as $Ni(CN)_4^{-2}$ (Eq. 4). The equilibrium constant for redissolution is very favorable (K_{eq} = 7.95 x 10^{12} M^{-1}).

$$Ni(OH)_{2\,(s)} + 4\,CN^- \rightleftarrows Ni(CN)_4^{-2} + 2\,OH^- \qquad (4)$$

Identification of soluble iron as $Fe(CN)_6^{-4}$ and soluble nickel as $Ni(CN)_4^{-2}$ allows a determination of cyanide balance. The preliminary value of 0.0155 *M* $Fe(CN)_6^{-4}$ in the 70°C starting solution gives an estimate of the starting moles of cyanide ion. The sum of the moles of cyanide bound to nickel and iron, using FTIR results, combined with the moles of ammonia measured, accounts for the starting cyanide within 10%, on the average. A refinement of the cyanide balance will be made when better reaction temperature solubility data are obtained.

2.3.2 Dependence of IF-1B Hydrolysis on Gamma Dose Rate

Last fiscal year, results of three sets of experiments were reported in which incident gamma dose rate was varied over one order of magnitude at 90°C. Table 2.4 summarizes the gamma dose rates used and other conditions of each experiment. Figure 2.13 shows some of those data along with new data collected at 2-3 and 5-6 days. Higher and more rapid conversion was obtained at higher dose rates.

As in the temperature-dependence experiments, the change in ammonia concentration with time is approximately linear (Figure 2.14). Again, no mechanism is implied or suggested by this assumption. Rate constants calculated from the slopes of the linear regression lines through the data are given in Table 2.3. A plot of rate constant as a function of gamma dose rate is linear (Figure 2.15) with a slope of 2.8 x 10^{-8} $M \cdot h \cdot Rad^{-1} \cdot day^{-1}$. The intercept gives a rate constant consistent with results of the

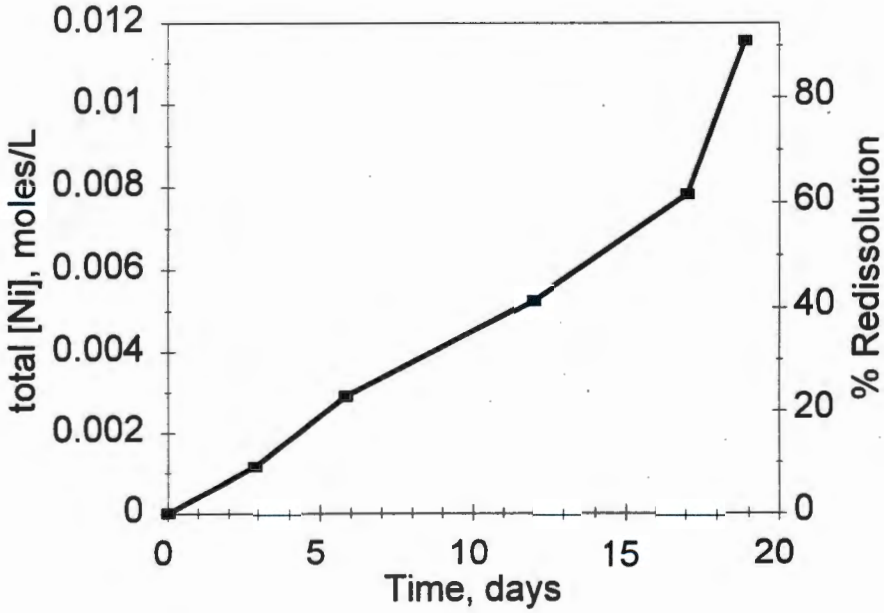

Figure 2.12. Total Nickel Concentration in the Hydrolysis of IF-1B (0.5 g) at 80°C and at a Gamma Dose Rate of 1.07 x 10^5 Rad/h (H10)

Table 2.4. Conditions for IF-1B Hydrolysis Experiments Investigating the Effect of Applied Gamma Dose Rate Variation. Experiments conducted in 25 mL of 2 *M* NaOH for 3 weeks.

Experiment Number	Gamma Dose Rate (Rad/h)	Weight IF-1B used (g)	Temperature (°C)
H1	1.07 x 10^5	0.5	90
H4	4.25 x 10^4	0.5	90
H5	8.91 x 10^3	0.5	90

non-irradiated control experiments at 90°C if the linear approximation is made, although this is a poor model for the thermal data (Figure 2.4). The gamma dose rate dependence of hydrolysis, therefore, can be described by Eq. (6), where γ is the incident gamma dose rate and $k_{\gamma,90}$ is the predicted hydrolysis rate constant at 90°C.

$$k_{\gamma,90} = 2.8 \times 10^{-8} \cdot \gamma + 7.88 \times 10^{-4} \quad (6)$$

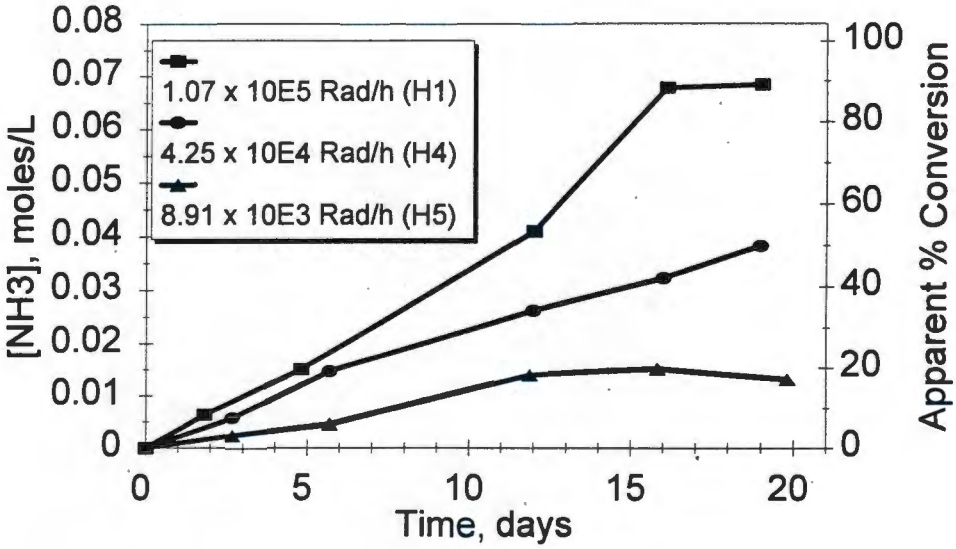

Figure 2.13. Applied Gamma Dose Rate Dependence of Ammonia Production in the Hydrolysis of IF-1B (0.5 g) at 90°C

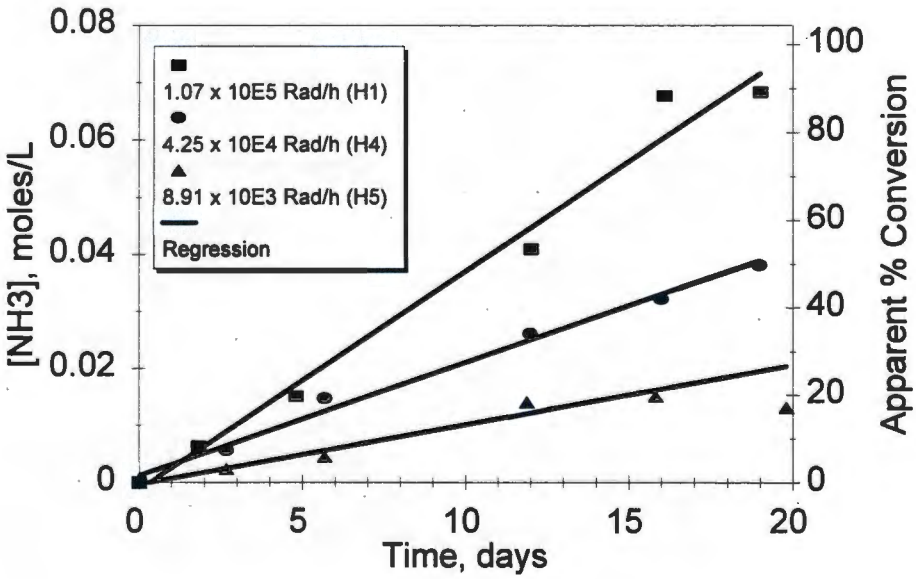

Figure 2.14. Linear Approximation to the Applied Gamma Dose Rate Dependence of Ammonia Production in the Hydrolysis of IF-1B (0.5 g) at 90°C

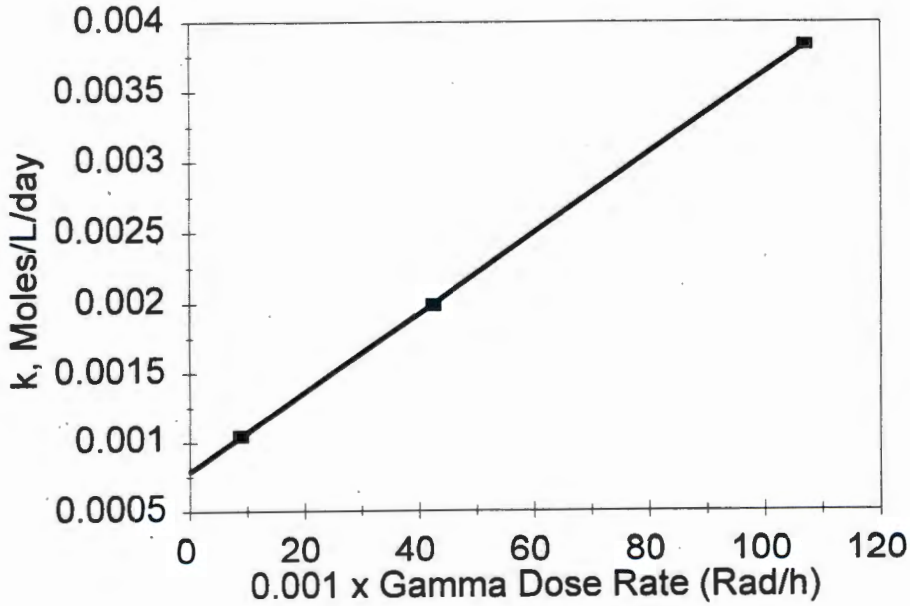

Figure 2.15. Ammonia Production Rate Constant as a Function of Applied Gamma Dose Rate in the Hydrolysis of IF-1B (0.5 g) at 90°C

The decrease in iron concentration in irradiated supernate solutions was modeled assuming pseudo-first-order behavior as for the temperature-dependence experiments. Calculated rate constants are listed in Table 2.3, and Figure 2.16 shows the fit to the data. Figure 2.17 shows that the rate constant of iron loss appears to decrease linearly with incident dose rate (initial rate data give a straight line with less scatter). The slope is 1.0×10^{-6} $day^{-1} \cdot h \cdot Rad^{-1}$ at 90°C. The intercept is very nearly 0, in agreement with the observation that the iron concentration does not decrease appreciably in control solutions over the 20-day period of the 90°C experiments.

A hydrolysis experiment was conducted at 100°C and 8.91×10^3 Rad/h. Ammonia production observed in this experiment is compared with other related experiments in Figure 2.18. As expected, the extent of hydrolysis was greater than in the 90°C experiment at the same dose rate, and less than that obtained in the higher dose rate experiment at the same temperature. It is not known why the Day-21 data point indicates a drop in ammonia produced, but the conversion shown is below that in the thermal control run under the same conditions (not shown), suggesting the Day-21 data may be in error. Ammonia radiolysis does occur, and, if hydrolysis slowed for some reason, such as if a more stable intermediate was formed, the ammonia concentration could drop. However, FTIR analysis of the Day-21 supernate shows that only $Fe(CN)_6^{-4}$ is present and does not offer an explanation for a decreased rate of conversion.

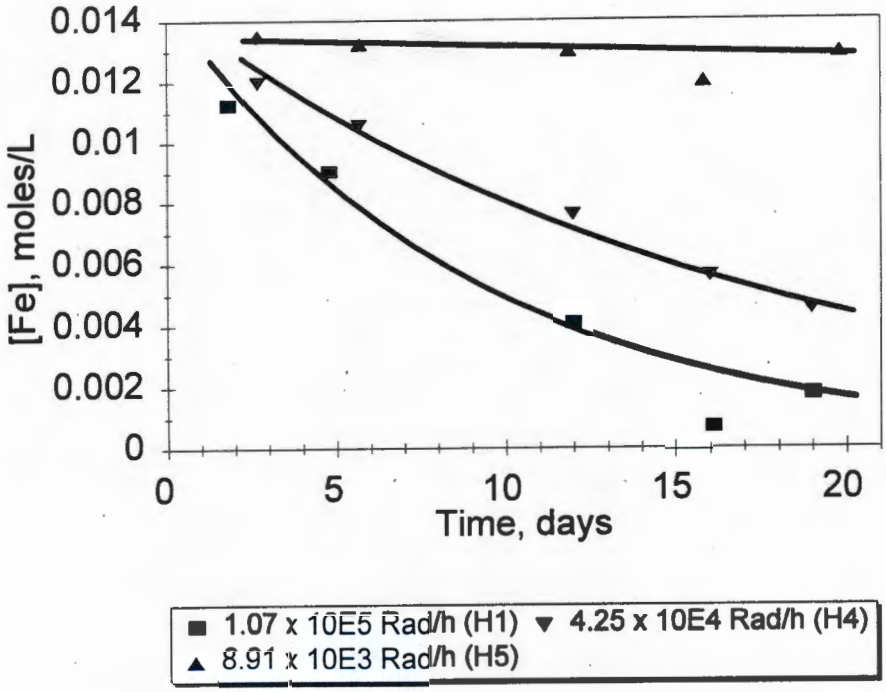

Figure 2.16. Decrease in Iron Concentration and Pseudo-First-Order Fit as a Function of Applied Gamma Dose Rate in the Hydrolysis of IF-1B (0.5 g) at 90°C

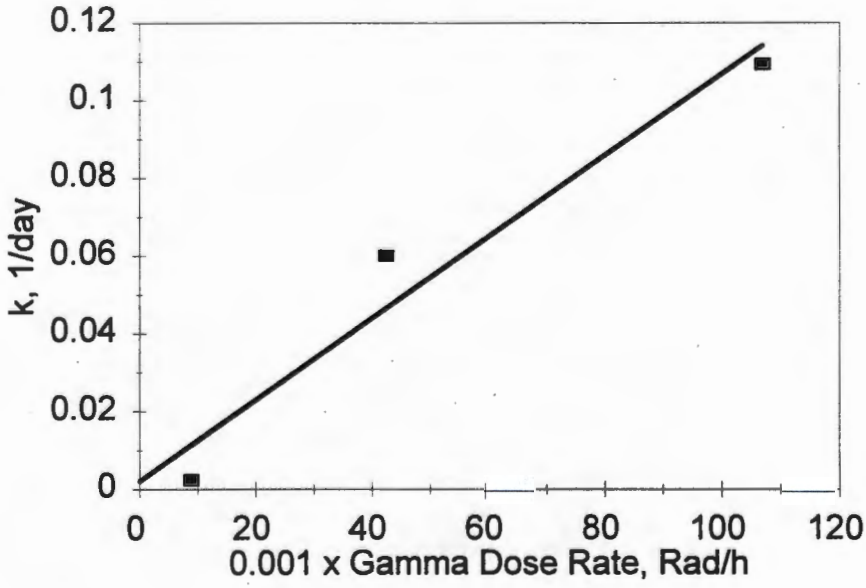

Figure 2.17. Iron Loss Rate Constant as a Function of Applied Gamma Dose Rate in the Hydrolysis of IF-1B (0.5 g) at 90°C

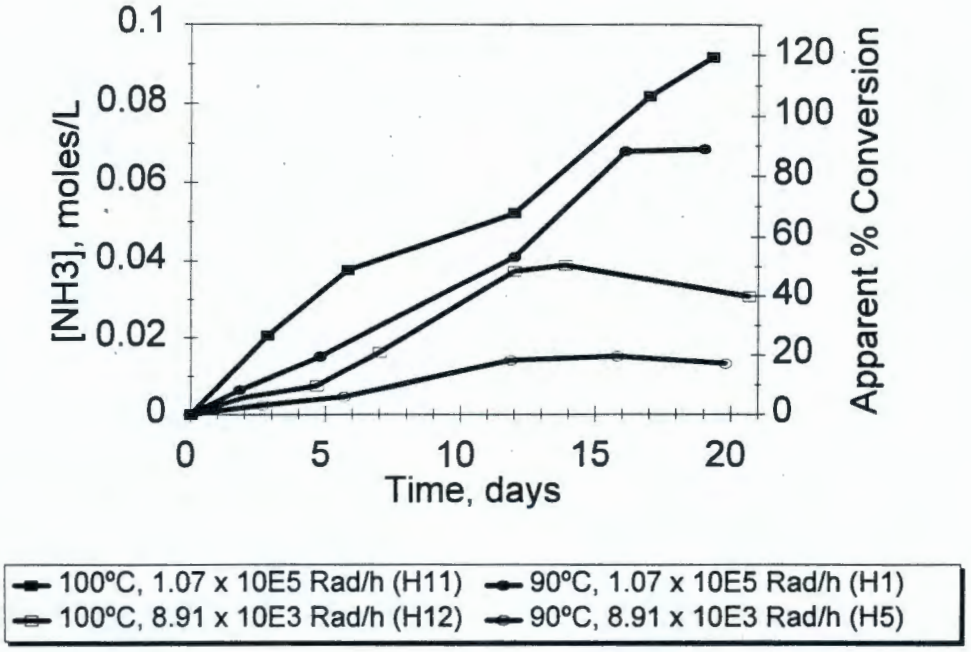

Figure 2.18. Ammonia Production During Hydrolysis of IF-1B in an Experiment in Which Both the Applied Gamma Dose Rate and Temperature Were Varied

If the linear approximation is made using all data except the Day-21 data, a rate constant for ammonia production of 3.0 x 10^{-3} *M*/day is obtained. This rate constant is in very good agreement with the predicted value of 3.6 x 10^{-3} *M*/day. This value was calculated by first using Eq. (6) to obtain a calculated rate constant at 90°C at the incident gamma dose rate, then adjusting to 100°C assuming that the temperature relationship of Eq. (5) held for the different gamma dose rate.

2.3.3 Influence of Added Metal Ions on IF-1B Hydrolysis

The influence of metal ions present in tank waste on In-Farm flowsheet material hydrolysis was investigated. These experiments were conducted using a similar methodology as experiments discussed in the previous sections, except thick-wall stainless steel vessels (0.93-cm wall thickness) were used and experiments were terminated and sampled after 13 days. Vessels were charged with 0.5 g of IF-1B ferrocyanide simulant, the metal to be tested, and 25 mL of 2 *M* NaOH solution. The vessels were purged with argon, sealed, irradiated at an applied gamma dose rate of about 1.07 x 10^5 Rad/h, and heated to 90°C. Controls in this set of experiments were prepared and handled identically, including gamma irradiation, except they did not contain the added metal ion.

Metal ions chosen for addition were Bi, Pb, Zn, and Cr because C-112 and C-109 tank sample analyses showed that these ions were present in more than trace level concentrations (Simpson, et al. 1993a; Simpson et al. 1993b). The maximum average concentrations of Cr and Zn in acid-digested

core composite analyses were 241 and 314 $\mu g/g$, respectively. Lead was present in higher concentrations with a maximum average concentration of 9238 $\mu g/g$ reported for acid-digested C-109 Core 47 composite. In hydrolysis studies, the concentration of metal ion used was 0.01 g/0.5 g simulant, or over 100 times the measured Cr and Zn concentrations and about twice the measured Pb concentration. The metal ions were added as $BiPO_4$, $Pb(NO_3)_2$, $Cr(NO_3)_3$, and $Zn(OH)_2$.

Aluminum is also a major component of tank waste and was investigated more thoroughly in FY 1994. Aluminum was found to have a minimal effect and may have slightly promoted hydrolysis. In addition, the influence and participation of nickel through the redissolution of $Ni(OH)_2$ have been discussed above. The hydrolysis of the redissolution product $Ni(CN)_4^{-2}$ is described in Section 2.4.

Figure 2.19 shows the results of the 13-day hydrolysis experiments with and without added metal ions, along with FY 1994 data from Experiment H1 that were collected under identical conditions in the same vessels. Pb, Cr, Bi, and Zn ions do not affect the extent of aging of the ferrocyanide flowsheet simulant, as indicated by the amount of ammonia produced after about 13 days in a gamma field. Results of experiments containing these ions were statistically the same as results from identical control experiments, which did not contain additives. Overall, metal ion and control data had a relative standard deviation of about 11%, which indicates the reproducibility of these experiments. The metal ion and control data are also consistent with a linear extrapolation of the H1 data.

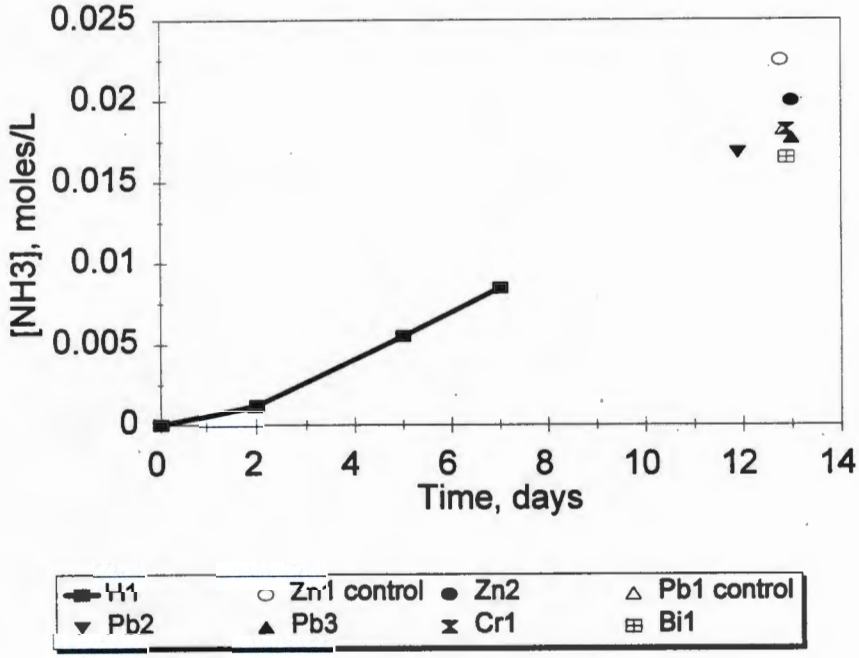

Figure 2.19. Influence of Added Metal Ions on Hydrolysis of IF-1B at 90°C with an Applied Gamma Dose Rate of 1.07 x 10^5 Rad/h

Analyses of the supernate solutions of the metal ion experiments showed that the metal ions were soluble to different extents (Bi, 2%; Cr, 16%; Pb, 67%; and Zn, 81% of the added metal ion dissolved), but the nature of the soluble species is not known. Zinc cyanide is reported to be more easily hydrolyzed than either nickel or iron cyanides (Robuck and Luthy 1989; Tan and Teo 1987) and, if formed, may have no observable influence. The observation that the metal ions were in the solution phase and yet had no appreciable effect on hydrolysis further suggests that these ions play no significant role in aging.

2.4 Hydrolysis of $K_2Ni(CN)_4$

The $Ni(CN)_4^{-2}$ anion was shown to be formed as an intermediate in the aging of IF-1B flowsheet material. This anion, detected in FTIR spectra of aged supernate solutions, was formed when $Ni(OH)_2$ was redissolved by CN^- liberated from $Fe(CN)_6^{-4}$ under hydrolysis conditions. Up to 90% redissolution was observed.

Hydrolysis of 0.0128 *M* $K_2Ni(CN)_4$ dissolved in 2 *M* NaOH was investigated at 90°C and 1.07×10^5 Rad/h. The results are compared on a mole% hydrolysis basis, as determined by moles of ammonia measured, with results of IF-1B hydrolysis under the same temperature and dose rate conditions (H1). Figure 2.20 indicates that, in the gamma pit, the rate of $Ni(CN)_4^{-2}$ hydrolysis is only slightly less than the rate for $Fe(CN)_6^{-4}$. However, the thermal control experiments show the opposite reactivity, with higher conversion of the $Ni(CN)_4^{-2}$ observed. It has been reported that nickel cyanide and ferrocyanide have similar thermal hydrolysis behavior (Robuck and Luthy 1989; Tan and Teo 1987).

2.5 Hydrolysis of IF-1B at 60°C and pH 10

Cesium scavenging was performed at a pH in the range of 8 to 10. If waste added subsequently did not mix thoroughly, or did not contact the sludge through convection (McGrail et al. 1993; McGrail 1994), areas within the ferrocyanide waste might never have been exposed to high pH and may not have been heated to a high temperature. In the experiments used to investigate the behavior of such waste, IF-1B (0.5 g) was contacted with a pH 10 carbonate buffer (25 mL) containing 0.77 *M* $NaNO_3$ (to give a 1 *M* $[Na^+]$ solution), gamma-irradiated at an incident dose rate of 4.5×10^4 Rad/h, and heated to 60°C. Four identically prepared solutions were irradiated and sampled individually over a 5.3-month period. Vessels used in this series were Monel with a wall thickness of 0.55 cm.

The change in ammonia concentration over the course of this experiment is shown in Figure 2.21. The concentration in the 161-day sample indicates an apparent cyanide conversion of about 18 mole%. The actual conversion is higher because ammonia radiolysis decreases the concentration with time. If it is assumed that ammonia production is linear with time, as assumed above, a global rate constant for ammonia production of 8.0×10^{-5} *M*/day is calculated. The fit of the data to the linear model is not very good, but this rate constant is similar to the rate constant determined for the 70°C experiment

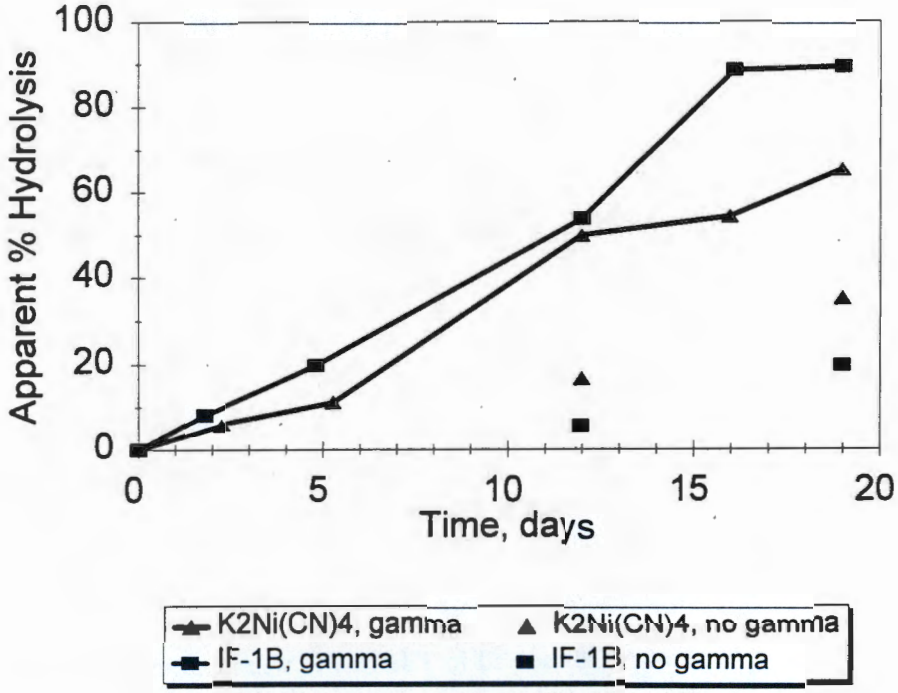

Figure 2.20. Ammonia Production During Hydrolysis of $K_2Ni(CN)_4$ in 2 *M* NaOH at 90°C with an Applied Gamma Dose Rate of 1.07 x 10^5 Rad/h

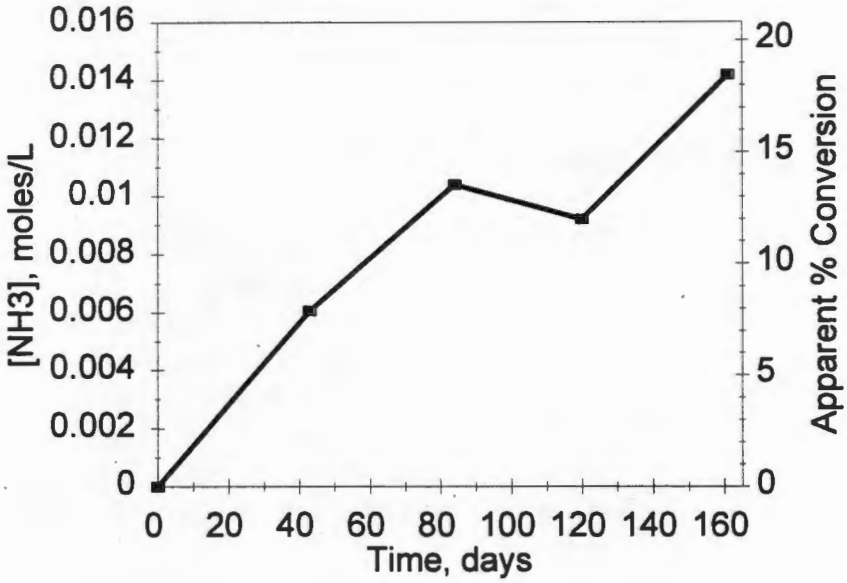

Figure 2.21. Ammonia Production During Hydrolysis of IF-1B at pH 10 and 60°C with an Applied Gamma Dose Rate of 4.5 x 10^4 Rad/h

conducted in 2 *M* NaOH. If Eq. (6) is used to calculate a rate constant at the applied gamma dose rate used in this experiment, then adjusted to 60°C using the relationship in Eq. (5), a rate constant of 3.3×10^{-5} *M*/day is calculated. Considering the low solubility of IF-1B in pH 10 solution, this value is in remarkably close agreement to the observed rate constant. The difference in pH may not greatly affect the hydrolysis reaction itself, since it is reported that thermal hydrolysis is unaffected above pH 9 (Kuhn and Rice 1977). It should be noted, however, that the calculation uses applied dose rates rather than absorbed dose rates, and differences in attenuation by the different vessels are not accounted for. Vessels in the long-term experiments had a thicker wall thickness (greater attenuation) than the vessels for which the correlation was devised.

THIS PAGE INTENTIONALLY
LEFT BLANK

3.0 Conclusions

The hydrolysis of ferrocyanide anion from In-Farm-1B, Rev. 7, an In-Farm flowsheet simulant, dissolved in 2 *M* NaOH has been investigated. The effects of gamma radiation (1.07×10^5, 4.25×10^4, and 8.91×10^3 Rad/h incident dose rate), temperature (50°C, 70°C, 80°C, 90°C, and 100°C), and metal ion additives were determined. Radiolysis (ammonia and formate) and hydrolysis [$Ni(CN)_4^{-2}$] of intermediates formed in the aging process were investigated. Also, a 5.3-month hydrolysis experiment was conducted in pH 10 solution at 60°C with an applied gamma dose rate of 4.5×10^4 Rad/h. Reactions were monitored as a function of time using analyses of soluble [NH_3], [Fe], [Ni], [Cs], [NO_3^-], [NO_2^-], and [HCO_2^-]. FTIR analysis was also used on selected supernate solutions.

Results of these and prior studies show that aging of simulated wastes in contact with highly caustic solutions does occur, resulting in the dissolution and hydrolysis of ferrocyanide ion. It is likely that any ferrocyanide-bearing sludge that came in contact with highly caustic waste could have undergone similar aging and may have become significantly depleted of ferrocyanide ion. The results also suggest that ferrocyanide waste not contacted by a highly caustic solution might also be destroyed in a gamma field.

In general, aging can be described by the following equations. Detailed mechanistic information, such as the nature of intermediate iron cyanide species, cannot be determined.

$$Na_2NiFe(CN)_{6\,(s)} + 2\,OH^- \rightleftarrows Fe(CN)_6^{-4} + 2\,Na^+ + Ni(OH)_{2\,(s)}$$

$$Fe(CN)_6^{-4} + x\,L^n \rightleftarrows Fe(CN)_{6-x}L^{-4+x(n+1)} + x\,CN^-$$

$L^n = OH^-, H_2O$, etc.

$$Ni(OH)_{2\,(s)} + 4\,CN^- \rightleftarrows Ni(CN)_4^{-2} + 2\,OH^-$$

$$CN^- + 2\,H_2O \rightleftarrows HCO_2^- + NH_3$$

Gamma radiation promoted the destruction of ferrocyanide anion by hydrolysis to ammonia and formate ion. Yields of ammonia were found to be higher in reaction solutions exposed to gamma radiation than in identical solutions that were not irradiated. As the gamma dose rate increased, the rate of hydrolysis also increased. Similarly, increasing temperature increased the rate of ammonia production. As an approximation, ammonia production with time was described as being linear, and rate constants for ammonia production were obtained from the slope of the lines. A linear Arrhenius relationship was obtained. The change in rate constant with applied gamma dose rate was also found to be linear. The temperature and dose rate relationships were used to predict rate constants for ammonia production at other conditions.

The total concentrations of all soluble iron species decreased in most gamma-irradiated solutions, apparently following a pseudo-first-order rate law. The calculated rate constants for this decrease correlated linearly with temperature and gamma dose rate. For both gamma-irradiated and control solutions, total iron concentrations determined by AA correlated well with ferrocyanide ion concentrations determined by FTIR, indicating that soluble iron is in the form of ferrocyanide ion.

Nickel, initially precipitated as $Ni(OH)_2$ when the flowsheet simulant reacts with aqueous base, is redissolved when free cyanide ion, liberated when ferrocyanide ion is destroyed, forms the $Ni(CN)_4^{-2}$ anion. This anion was identified in FTIR spectra of supernate solutions. $Ni(CN)_4^{-2}$ was found to hydrolyze at a slightly slower rate than ferrocyanide anion in a gamma field.

Hydrolysis occurs faster than expected at 60°C in a pH 10 solution. In the gamma field, an ammonia yield of at least 18 mole% was obtained. The rate constant obtained by assuming linear ammonia production is very similar to the rate constant determined for the 70°C, 2 *M* NaOH experiment and could be reasonably approximated using temperature and dose rate relationships developed from experiments conducted in 2 *M* NaOH. The rate constant obtained is unexpectedly high, considering the low solubility of $Na_2NiFe(CN)_6$ at this pH, and may indicate that even ferrocyanide sludge that did not come into direct contact with highly basic wastes may also have aged significantly.

Continuing studies will provide more information about aging of relatively insoluble cesium nickel ferrocyanides. Further work is planned on the temperature and gamma dependence of $Ni(CN)_4^{-2}$ hydrolysis. A study of the properties and energy content of aged materials in comparison with reported tank sample data is planned. Also planned are solution dosimetry experiments conducted in the various vessels used in these experiments so that correlations may be more properly expressed in terms of absorbed dose rate rather than incident dose rate. Isotopic labeling studies are scheduled to determine radiolysis products of formate ion.

4.0 References

Anderson, J. D. 1990. *A History of the 200 Area Tank Farms.* WHC-MR-0132, Westinghouse Hanford Company, Richland, Washington.

Borsheim, G. L., and B. C. Simpson. 1991. *An Assessment of the Inventories of the Ferrocyanide Watchlist Tanks*. WHC-SD-WM-ER-133 Rev. 0, Westinghouse Hanford Company, Richland, Washington.

Bryan, S. A., K. H. Pool, S. L. Bryan, R. L. Sell, and L.M.P. Thomas. 1993. *Ferrocyanide Safety Program. Cyanide Speciation Studies FY 1993 Annual Report.* PNL-8887, Pacific Northwest Laboratory, Richland, Washington.

Burger, L. L. 1984. *Complexant Stability Investigation, Task 1 - Ferrocyanide Solids*. PNL-5441, Pacific Northwest Laboratory, Richland, Washington.

Burger, L. L., and R. D. Scheele. 1988. *Interim Report - Cyanide Safety Studies*. PNL-7175, Pacific Northwest Laboratory, Richland, Washington.

Burger, L. L., and R. D. Scheele. 1991. *The Reactivity of Cesium Nickel Ferrocyanide Towards Nitrate and Nitrite Salts - A Status Report*. PNL-7550, Pacific Northwest Laboratory, Richland, Washington.

Burger, L. L., D. A. Reynolds, W. W. Schulz, and D. M. Strachan. 1991. *A Summary of Available Information on Ferrocyanide Tank Wastes*. PNL-7822, Pacific Northwest Laboratory, Richland, Washington.

Cady, H. H. 1993. *Evaluation of Ferrocyanide/Nitrate Explosive Hazard.* LA-12589-MS, Pacific Northwest Laboratory, Richland, Washington.

Crowe, R. D., M. Kummerer, and A. K. Postma. 1993. *Estimation of Heat Load in Waste Tanks Using Average Vapor Space Temperatures.* WHC-EP-0709, Westinghouse Hanford Company, Richland, Washington.

Deaton, D. E. 1990. *Unusual Occurrence-Unreviewed Safety Questions Regarding Tanks Containing Ferrocyanide.* WHC-90-B003-R1, Update 10-22-90, Westinghouse Hanford Company, Richland, Washington.

Dodds, J. N., and W. J. Thompson. 1994. "DXRD Studies of Sodium Nickel Ferrocyanide Reactions with Equimolar Nitrate/Nitrite Salts." *Environ. Sci. Technol.* 28(5):882-889.

Epstein, M., and H. K. Fauske. 1994. *Conditions for Reaction Propagation in Dried Ferrocyanide/Nitrate-Nitrite Powders*. WHC-SD-WM-TI-619, Rev. 0, Westinghouse Hanford Company, Richland, Washington.

Goldstein, S., G. Czapski, H. Cohen, and D. Meyerstein. 1988. "Formation and Decomposition of Iron-Carbon σ-Bonds in the Reaction of Iron(III)-Poly(amino carboxylate) Complexes with CO_2^- Free Radicals. A Pulse Radiolysis Study." *J. Am. Chem. Soc.* 110(12):3903-3907.

Hallen, R. T., L. L. Burger, R. L. Hockey, M. A. Lilga, R. D. Scheele, and J. M. Tingey. 1992. *Ferrocyanide Safety Project FY 1991 Annual Report*. PNL-8165, Pacific Northwest Laboratory, Richland, Washington.

Hepworth, J. L., E. D. McClanahan, and R. L. Moore. 1957. *Cesium Packaging Studies - Conversion of Zinc Ferrocyanide to a Cesium Chloride Product*. HW-48832, Hanford Atomic Products Operation, Richland, Washington.

Jeppson, D. W., and J. J. Wong. 1993. *Ferrocyanide Waste Simulant Characterization*. WHC-EP-0631, Westinghouse Hanford Company, Richland, Washington.

Kuhn, A., and C. Rice. 1977. "Alkaline Hydrolysis of Cyanides, Cyanates, and Dicyan." *Oberflache-Surface* 18:119-123.

Lilga, M. A., M. R. Lumetta, W. F. Riemath, R. A. Romine, and G. F. Schiefelbein. 1992. *Ferrocyanide Safety Project, Subtask 3.4, Aging Studies FY 1992 Annual Report*. PNL-8387, Pacific Northwest Laboratory, Richland, Washington.

Lilga, M. A., M. R. Lumetta, and G. F. Schiefelbein. 1993. *Ferrocyanide Safety Project, Task 3 Ferrocyanide Aging Studies FY 1993 Annual Report*. PNL-8888, Pacific Northwest Laboratory, Richland, Washington.

Lilga, M. A., E. V. Alderson, D. J. Kowalski, M. R. Lumetta, and G. F. Schiefelbein. 1994. *Ferrocyanide Safety Project, Task 3 Ferrocyanide Aging Studies FY 1994 Annual Report*. PNL-10126, Pacific Northwest Laboratory, Richland, Washington.

McGrail, B. P. 1994. *Computational Analysis of Coupled Fluid, Heat, and Mass Transport in Ferrocyanide Single-shell Tanks: FY 1994 Interim Report. Ferrocyanide Tank Safety Project*. PNL-10163, Pacific Northwest Laboratory, Richland, Washington.

McGrail, B. P., D. S. Trent, G. Terrones, J. D. Hudson, and T. E. Michener. 1993. *Computational Analysis of Fluid Flow and Zonal Deposition in Ferrocyanide Single-Shell Tanks*. PNL-8876, Pacific Northwest Laboratory, Richland, Washington.

McLaren, J. M. 1993. *Ferrocyanide Safety Program: Updated Thermal Analysis Model for Ferrocyanide Tanks with Application to Tank 241-BY-104.* WHC-EP-0669, Westinghouse Hanford Company, Richland, Washington.

McLaren, J. M. 1994. *Ferrocyanide Safety Program: Thermal Analysis of Ferrocyanide Tanks, Group I.* WHC-EP-0729, Westinghouse Hanford Company, Richland, Washington.

McLaren, J. M., and R. J. Cash. 1993. *Ferrocyanide Safety Program: Heat Load and Thermal Characteristics Determination for Selected Tanks.* WHC-EP-0638, Westinghouse Hanford Company, Richland, Washington.

Meacham, J. E., R. J. Cash, and G. T. Dukelow. 1994a. *Quarterly Report on the Ferrocyanide Safety Program for the Period Ending June 30, 1994.* WHC-EP-0474-13, Westinghouse Hanford Company, Richland, Washington.

Meacham, J. E., R. J. Cash, G. T. Dukelow, H. Babad, and J. W. Buck. 1994b. *Data Requirements for the Ferrocyanide Safety Issue Developed Through the Data Quality Objectives Process.* WHC-SD-WM-DQO-007, Westinghouse Hanford Company, Richland, Washington.

Peach, J. D. 1990. "Consequences of Explosion of Hanford's Single-Shell Tanks Are Understated." Letter B-241479 dated October 1990 to M. Synar, GAO/RCED-91-34, General Accounting Office, Washington, D.C.

Postma, A. K., J. E. Meacham, G. S. Barney, G. L. Borsheim, R. J. Cash, M. D. Crippen, D. R. Dickinson, J. M. Grigsby, D. W. Jeppson, M. Kummerer, J. M. McLaren, C. S. Simmons, and B. C. Simpson. 1994. *Ferrocyanide Safety Program: Safety Criteria for Ferrocyanide Watch List Tanks.* WHC-EP-0691, Westinghouse Hanford Company, Richland, Washington.

Robuck, S. J., and R. G. Luthy. 1989. "Destruction of Iron-Complexed Cyanide by Alkaline Hydrolysis." *Wat. Sci. Tech.* 21:547-558.

Scheele, R. D., and H. H. Cady. 1992. *Preliminary Safe-Handling Experiments on a Mixture of Cesium Nickel Ferrocyanide and Equimolar Sodium Nitrate/Nitrite.* PNL-7928, Pacific Northwest Laboratory, Richland, Washington.

Scheele, R. D., L. L. Burger, J. M. Tingey, S. A. Bryan, G. L. Borsheim, B. C. Simpson, R. J. Cash, and H. H. Cady. 1991. "Ferrocyanide-Containing Waste Tanks: Ferrocyanide Chemistry and Reactivity." PNL-SA-19924, presented at *Environmental Restoration 1991*, University of Arizona, Tucson, Arizona.

Scheele, R. D., L. L. Burger, J. M. Tingey, R. T. Hallen, and M. A. Lilga. 1992. "Chemical Reactivity of Potential Ferrocyanide Precipitates in Hanford Tanks with Nitrates and Nitrites." In *Proceedings of Waste Management '92*, Tucson, Arizona.

Simpson, B. C., G. L. Borsheim, and L. Jensen. 1993a. *Tank Characterization Data Report: Tank 241-C-112.* WHC-EP-0640, Rev. 1, Westinghouse Hanford Company, Richland, Washington.

Simpson, B. C., G. L. Borsheim, and L. Jensen. 1993b. *Tank Characterization Report: Tank 241-C-109.* WHC-EP-0668, Westinghouse Hanford Company, Richland, Washington.

Tan, T. C., and W. K. Teo. 1987. "Destruction of Cyanides by Thermal Hydrolysis." *Plating and Surface Finishing* 74:70-73.

U.S. Department of Energy (DOE). 1987. *Final Environmental Impact Statement, Disposal of Hanford Defense High-Level, Transuranic, and Tank Wastes.* DOE-EIS-0113, Washington, D.C.

9613457.1135

Distribution

No. of
Copies

OFFSITE

Charles S. Abrams
1987 Virginia
Idaho Falls, ID 83404

Shirley Campbell-Grizzel
U.S. Department of Energy
EH-15, Trevion II
12800 Middlebrook Road
Germantown, MD 20874

Cynthia Hilland
U.S. Department of Energy
656 Quince Diamond Road
Room 235, EM-20.1
Gaithersburg, MD 20879

George E. Schmauch
Air Products & Chemicals, Inc.
7201 Hamilton Blvd.
Allentown, PA 18195-1501

Kamal K. Bandyopadhyay
Brookhaven National Laboratory
Upton, NY 11973

David O. Campbell
102 Windham Road
Oak Ridge, TN 37830

Fred N. Carlson
6965 North 5th West
Idaho Falls, ID 83401

No. of
Copies

Gary Powers
Design Science, Inc.
163 Witherow Road
Sewickley, PA 15143

2 Fauske and Associates, Inc.
16W070 W. 83rd St.
Burr Ridge, IL 60521
Hans K. Fauske
Michael Epstein

Gregory R. Choppin
Florida State University
Department of Chemistry B-164
Tallahassee, FL 32306

Melvin W. First
Harvard University
295 Upland Avenue
Newton Highlands, MA 02161

Chester Grelecki
Hazards Research Corporation
200 Valley Road, Suite 301
Mt. Arlington, NJ 07856

Billy Hudson
202 Northridge Court
Lindsborg, KA 67456

Thomas S. Kress
102-B Newridge Road
Oak Ridge, TN 37839

No. of
Copies

2 Los Alamos National Laboratory
P.O. Box 1663
Los Alamos, NM 87545
Steve F. Agnew
Thomas E. Larson

Mujid S. Kazimi
MIT/Dept of Nuclear Eng.
77 Massachusetts Avenue
Room 24-102
Cambridge, MA 02139

J. Louis Kovach
Nuclear Consulting Services, Inc.
P.O. Box 29151
Columbus, OH 43229-0151

2 Oak Ridge National Laboratory
P.O. Box 2008
Oak Ridge, TN 37831
Emory D. Collins, MS-6385
Charles W. Forsberg, MS-6495

2 G & P Consulting, Inc.
3640 Ballard Road
The Dalles, OR 97338
Arlin K. Postma
J. Michael Grigsby

William R. Prindle
1556 Crestline Drive
Santa Barbara, CA 93105

Andrew S. Veletsos
Rice University
5211 Paisley
Houston, TX 77096

No. of
Copies

2 Sandia National Laboratory
P.O. Box 5800
Albuquerque, NM 87185
Scott E. Slezak, MS-0741
Dana Powers, MS-0744

Alfred Schneider
5005 Hidden Branches Drive
Dunwoody, GA 30338

3 Ray S. Daniels (3)
Science Applications International
Corporation
20300 Century Blvd., Suite 200-B
Germantown, MD 20874

Michael T. Gordon
State of Washington
Department of Ecology
P. O. Box 47600
Olympia, WA 98504-7600

Alex Stone
1315 W. 4th Avenue
Kennewick, WA 99336

6 U.S. Department of Energy
EM-36, Trevion II
12800 Middlebrook Road
Germantown, MD 20874
James V. Antizzo
Charles O'Dell (5)

Thomas C. Temple
U.S. Department of Energy
Savannah River Operations Office
P.O. Box A
Aiken, SC 29808

No. of
Copies

Bruce R. Kowalski
University of Washington
Center for Process Analytical Chemistry
Chemistry Department BG-10
Seattle, WA 98195

Joseph S. Byrd
University of South Carolina
Department of Electrical and Computer Engineering
Swearingen Engineering Center
Columbia, SC 29208

Frank L. Parker
Vanderbilt University
P.O. Box 1596, Station B
Nashville, TN 37235

Donald T. Oakley
Waste Policy Institute
555 Quince Orchard Road, Suite 600
Gaithersburg, MD 20878-1437

FOREIGN

Claude Musikas
Consultant
5, Avenue Moissan,
91440 Bures/Yvette,
France

No. of
Copies

ONSITE

10 **U.S. Department of Energy Richland Operations Office**

R. E. Gerton, S7-54
R. G. Harwood, S7-54
W. F. Hendrickson, S7-54
D. H. Irby, S7-54 (2)
M. F. Jarvis, S7-54
A. G. Krasopoulos, A4-81
Public Reading Room, H2-53
RL Docket File, B1-17 (2)

40 **Westinghouse Hanford Company**

H. Babad, S7-30
G. S. Barney, T5-12
J. B. Billetdeaux, S7-16
D. C. Board, S1-57
W. S. Callaway, X2-10
R. J. Cash, S7-15 (5)
M. D. Crippen, L5-31
R. D. Crowe, H0-38
D. R. Dickinson, L5-31
G. T. Dukelow, S7-15
D. L. Herting, T6-09
M. N. Islam, R3-08
D. W. Jeppson, L5-31
N. W. Kirch, R2-11
C. A. Kuhlman, B3-30
E. J. Lipke, S7-14
L. L. Lockrem, S3-90
N. G. McDuffie, S7-15
J. M. McLaren, H0-34
J. E. Meachann, S7-15 (2)
N. J. Milliken, H4-62
S. R. Moreno, B3-06
J. C. Person, T6-09

No. of
Copies

T. V. Rebagay, T6-30
F. R. Reich, L5-55
D. A. Reynolds, R2-11
E. F. Riedel, S3-90
B. C. Simpson, R2-12
H. Toffer, H0-38
W. T. Watson, H0-38
W. D. Winkelman, L5-55
W. D. Wittekind, H0-38
Central Files, L8-04
Correspondence Control, R1-20
EDMC, H6-08

34 **Pacific Northwest Laboratory**

E. G. Baker, P8-38
J. W. Brothers, K5-22

No. of
Copies

S. A. Bryan, K5-82
D. M. Camaioni, K2-44
J. A. Campbell, P8-08
S. R. Gano, P8-38
R. T. Hallen, P8-38 (2)
M. O. Hogan, P8-38
T. L. Hubler, P8-38
M. A. Lilga, P8-38 (10)
G. J. Lumetta, P7-25
M. R. Lumetta, P8-38
L. R. Pederson, K2-44
W. D. Samuels, K2-44
R. D. Scheele, P7-25
C. W. Stewart, K7-15
M. R. Telander, P8-44
Information Release (7)